Master Thesis in Geographical Information Science nr 65

3D geologic subsurface modeling within the Mackenzie Plain, Northwest Territories, Canada

NADINE RASKA

2017
Department of
Physical Geography and Ecosystem Science
Centre for Geographical Information Systems
Lund University
Sölvegatan 12
S-223 62 Lund
Sweden

Advisor: David Tenenbaum
Master degree project 30 credits in Geographic Information Sciences, 2017
Department of Physical Geography and Ecosystem Science, Lund University
Thesis nr 65

3D geologic subsurface modeling within the Mackenzie Plain, Northwest Territories, Canada

---

Nadine Raska

Master thesis, 30 credits, in Geographical Information Sciences

Supervisor

David Tenenbaum,

Lund University

Local Supervisor

Karen Fallas,

Geological Survey of Canada

Abstract

Three-dimensional (3D) models are widely used within the geosciences to provide scientists with conceptual and quantitative models of the earth's subsurface. As a result, 3D geologic modelling is a growing field, such that scientific research often cannot keep up with technical advancements. Literature often shows conflicting results with respect to which interpolation algorithms produce the best surfaces, and it is not always clear which methods are most appropriate for a particular geological setting.

This study looks at three commonly used interpolation techniques – Inverse Distance Weighting (IDW), kriging and triangulation – and assesses their effectiveness at capturing geologic structures in the subsurface. The study uses a modified Horizons method to create a solid 3D stratigraphic model of the subsurface of an area within the Mackenzie Plain, NWT, in Canada.

The Horizons method involves interpolating individual stratigraphic surfaces, or horizons, representing their depositional sequence. Surface intersections are corrected where necessary, and a solid model is built by extruding each surface down to the top of the surface below.

Triangulation produced the most geologically appropriate surfaces, whereas IDW produced surfaces with a stronger bullseye effect; although kriging produced some surfaces well, it did not result in acceptable surfaces where discontinuities were present. Structural features such as folds in the subsurface were captured only where the data density was sufficient. Large folds spanning the majority of the study area were visible in the modelled surfaces; however smaller folds and monoclines were not visible. It was possible to model a thrust fault in the subsurface by creating two separate stratigraphic models on either side of the fault, cutting them at the fault plane and merging them together after each side was converted to a solid model.

The model produced in this study showed promise as a basis for future modelling and further 3D model refinements. The modelling process was capable of highlighting areas where surface mapping did not match up with subsurface measurements, and conversely, highlighted areas where subsurface measurements did not match with

observed surface features. However, comparing the modelled results with seismic survey images in the region showed that the specific locations of the subsurface structures (e.g. fold troughs) were not captured in the correct location. As well, the presence of discontinuous surfaces made it necessary for manual edits to be performed, in order to accurately represent the known subsurface geology – complicating the model and making replicability more difficult.

The results presented in this thesis can be used to guide methods in other similar 3D modelling exercises. As well, it will help us apply the most appropriate methods for any given geologic setting, resulting in more accurate and efficient 3D models.

Keywords: Geography, Geographic Information Systems, 3D Modeling, Geology, Horizons, Stratigraphic Modeling

Acknowledgements

A huge thank you goes out to Lund University, the Geological Survey of Canada, my friends and family; you have all played your part in making this possible and I could not have done it without you.

To my supervisor at Lund University, David Tenenbaum, thank you for providing me with comments from across the ocean and several time zones away.

At the Geological Survey of Canada (GSC), I would like to thank first and foremost, Karen Fallas, for making this entire thesis possible. Your support and guidance on this thesis, as well as over my entire career at the GSC, has been invaluable. As well, Larry MacDonald – I tried my best to refrain from dragging you out of retirement for this one – but your help and guidance since I was an undergraduate just starting out with GIS, deserves recognition and has meant a lot to me. I would also like to thank the colleagues I have had the pleasure of working with at the GSC, particularly Glen Stockmal, Rob MacNaughton, you all helped me in some way.

A huge thank you goes to my family and friends. To Anne Farineau, for the mental support and doing it all before me, to Roho for your seemingly never-ending patience, and finally, to my parents, who always provide support in any way possible. Mom, how do I say "thank you" in a more intelligent way?

Support for this research by the Geological Survey of Canada (GSC) as a contribution to the Mackenzie Project of the Geo-Mapping for Energy and Minerals (GEM) Program, is gratefully acknowledged.

TABLE OF CONTENTS

1.0 INTRODUCTION

Understanding the subsurface of our earth is important for many different applications within the geosciences. The creation of three-dimensional models can assist with this understanding by providing us with a conceptual and quantitative model of the subsurface. These models assist with not only understanding the geologic evolution of the land, but with more specific applications such as mineral resource exploration, groundwater modelling or geothermal reservoir modelling.

1.1 Background to Geological Modelling

Geologic structures exist in the real world in three spatial dimensions, yet they are typically represented on a paper map in two dimensions. Geologists collect information from bedrock exposed at the surface to create drawings and maps of geological relationships. In areas where direct observations are absent, deduction of the structures must be performed. These deductions are based on a variety of complex relationships of nearby observations or measurements, as well as regional knowledge. Given that the subsurface is not directly observed, except via drilling holes, geologists have to use these other methodologies or acquisition methods to interpret the subsurface. Traditionally, this was accomplished through cross sections of the geologic subsurface, or maps of the tops and bottoms of the strata (Berg et al., 2011). However, this sort of two-dimensional view lacks the complexity and spatial relationships that three-dimensional (3D) models have. True 3D models can be used as means of improving geologic interpretations and potentially reveal inconsistencies in the cross-sections, resulting in a more complete and accurate interpretation (Caumon et al., 2009). Not only do 3D models help scientists conceptualize and see the subsurface in a realistic manner, they also allow scientists to more easily communicate complex geology in a simple, intuitive way, to both other professionals and the general public alike.

3D models are particularly useful for the management and extraction of natural resources, such as within the oil and gas industry. Building 3D models of the geologic subsurface is important not only to predict the location of prospective reservoirs, but to also predict and optimize various hydrocarbon recovery scenarios. These geological models and reservoir simulations help identify optimal field development scenarios and reduce exploration risk (Gundesø & Egeland, 1990; Labourdette et al. 2008). With

advancements in technology, largely due to the implementation of 3D seismic surveys by industry, subsurface visualization has come a long way (Fernandez et al. 2004).

Exploration success in the petroleum industry relies on effective visualization of the subsurface geological relationships. Information about the subsurface is acquired through reflection seismic data and petroleum exploration wells. For that reason, they have been drivers of 3D software development and tools have been directed towards visualizing subsurface relationships and reservoirs (Kessler et al., 2008). Seismic data provides the most continuous detail across an area and allows us to "see" features in the subsurface. In most other regional bedrock mapping efforts, usually by government geological surveys, such dense descriptive data is not always available and data is typically sparse. The private sector datasets are not always accessible to other users (Russell et al., 2015). In addition, the creation of customized programs, often created for such reservoir models, is not possible for everyone, due to the resources required to create customized programs. The most accessible data sources useful for 3D model creation include geological survey records (boreholes and outcrop and/or structural information collected during fieldwork), geological maps and cross-sections (Kauffman and Martin, 2008).

These geologic observations and interpretations performed by geologists are on-going, as our ability to view features, that were previously invisible to the naked eye, continues to develop. Geologists integrate many different types of information and data to perform interpretations across areas of sparse data. Consequently, there is no one modelling tool or software that can efficiently store, manipulate and publish everything that is needed. A combination of GIS tools, 3D modelling software and an appropriate database, will allow scientists to create comprehensive and useful 3D geologic models. Testing alternate methodologies and identifying limitations in both the modelling process and data gaps remains an important area of research in today's geospatial/geoscience world.

1.2 The Mackenzie Plain

The "Mackenzie Plain" is a low-lying physiographic region on either side of the Mackenzie River, between the Mackenzie Mountains and the Franklin Mountains, in the Northwest Territories of Canada (Figure 3.1 in Section 3). Proterozoic to Cretaceous sedimentary strata underlie the Mackenzie Plain and these strata have been deformed

by folds and faults that formed in Late Cretaceous to Paleocene time, when the Mackenzie and Franklin Mountains formed (Aitken and Cook, 1974). This area has shown promise for petroleum resource potential, due to several large oil and gas field discoveries and numerous proven and potential source rocks which are present throughout the sedimentary succession (Dixon et al., 2007). Confirmed oil seeps were first seen in the late 1800s by the Geological Survey of Canada and more have been recorded since (Stewart, 1948). After nearly a century of oil and gas exploration, the Mackenzie Plain and surrounding area provides a rich archive of public-domain subsurface data from industry reflection seismic and drilling activities. Government surveys and universities have produced numerous geological observations from outcrops and measured sections (Fallas et al., 2015). The building blocks for 3D visualization/modelling – such as digital surface and subsurface bedrock data – are largely available in this region. The ability to integrate and display all these constraints in a single 3D view is a key for enhancing insight into the subsurface geology of the region, and for informed decision making.

1.3 Research Problem

Although industry is present in the Mackenzie Plain, no detailed, regional 3D stratigraphic models have been published and methodologies have not been created, or tested, to support regional stratigraphic mapping in this region. The general aim of this study is to apply 3D mapping methodologies to create a geologically accurate 3D subsurface model of the stratigraphy in the central Mackenzie Plain.

Building off this model in the Mackenzie Plain, we will assess the effectiveness of different interpolation algorithms in producing accurate stratigraphic geologic models, which include areas of faulting and folding. Commonly used methods for geologic applications include inverse distance weighting (IDW), kriging and triangulation (Russell et al., 2011). Their performance will be qualitatively assessed in the context of stratigraphic modelling in this specific region. In addition, the performance of these standard interpolation methods will be tested in areas of poorly distributed field observations, particularly in areas of more complex geological structures.

Finally, the assessment of accuracy remains an issue in 3D modelling. Most presented geologic models do not support anything more than a visual, qualitative uncertainty analysis, as there is no comprehensive, universally accepted measure to assess

uncertainties in a geologic model (Lelliott et al., 2009). Still, at least some measure of the uncertainty is necessary for end-users to understand the limitations of the built model (Turner, 2006). There have been several methodologies suggested, from complex geostatistical to highly qualitative ones (Wellman et al., 2010; Tacher et al., 2006). In this study, a simple qualitative assessment will be performed, as more complicated assessments are large undertakings on their own, and beyond the scope of this study.

This type of modelling work is applicable to many other regions where similar geologic conditions and sampled observations exist. In addition it could be used as a basis for more detailed subsurface mapping.

1.3.1 Research Objectives

The overall objective of this study is to develop methods that will contribute to clarifying the geological framework and basin evolution of the Mackenzie Plain area. This will be done by developing methods and techniques that will model the subsurface of the Mackenzie Plain in three-dimensions. In doing so, we also aim to provide insight into 3D geologic subsurface modeling methodologies and results assessments, that could be used in areas of similar geological setting and data inputs.

Specific objectives include:

- To develop a 3D subsurface model of an area within the Mackenzie Plain
- To assess and provide recommendations for improved techniques and suitable methodologies for 3D modelling of geologic features, with emphasis on the Mackenzie Plain and geologically similar areas
- To explore and develop methods of assessing results in 3D geologic models

1.3.2 Research Questions

The research objectives will be met by answering the following questions:

1. Using mapped surface geology and sparse boreholes, can we use a modified version of the Horizons Method (Lemon and Jones, 2003) to model the subsurface?

2. What does the subsurface of our study area in the Mackenzie Plain look like in three dimensions, using the methodology above?
3. What kind of input data can help constrain the spatial location of key geologic structures such as faults and folds?
4. What is the most suitable algorithm for interpolating stratigraphic surfaces, given the data available and geologic structures being represented?
5. What are the significant identifiable sources of error in the model, and how can we mitigate them?

2.0 LITERATURE REVIEW

Over the past decade, 3D geological modelling has made vast improvements, largely due to the implementation of 3D seismic surveying by industry, and advances in computer technology (Fernandez et al., 2004). The inputs to a geological model can vary widely by project. Consequently, the specific methods used for modelling can also vary. Not only do the inputs change the modelling technique, but the depositional environment and geologic structures present can as well. The wide array of papers written by different authors presenting different techniques reflects these considerations. It is not the focus of this paper to provide a comprehensive list of the different techniques possible. Therefore, only those most relevant to the research and type of modelling performed in this study are presented.

2.1 3D Modelling Methods and Considerations

The first consideration in a 3-dimensional modeling process is the inputs to the process. Kaufmann and Martin (2008) provide a good overview of the types of data typically input into a 3D geology model. They also propose methods and standards for the pre-processing stage of these data types - that is, structuring and storing them in digital formats.

Research has also been focused on how to model areas where limited data exists (Sprague and de Kemp, 2005; Calcagno et al., 2008). Natali et al. (2013) presents modelling methods for 3 different types of modeling scenarios; data-free, sparse-data and data-dense. Data-free and sparse-data scenarios are, understandably, the most difficult to model well. Hence, many authors have attempted to develop tools to do so. Calcagno et al. (2008) created a methodology that would model subsurface geology, including faults, from sparse datasets, using a potential field interpolation. Sprague and De Kemp (2005) tested and developed methods using Bézier techniques and a special form of splining (NURBS), from sparse spatial and structural datasets. However, it is acknowledged that this type of modelling still remains largely an interpretation of the data, performed by the user, and no ideal solution for modeling sparse data exists.

The specific modelling methods chosen will also vary based on the defined inputs. Different techniques are used when, for example, boreholes are the primary input (Zhu et al., 2012), or cross sections (Keller et al., 2011), a combination of the two (Lemon

and Jones, 2003), or even via surface mapping only (Dhont et al., 2005). In addition to the inputs, the geologic setting and type of geological system will influence the methods chosen. Turner (2006) provides a comprehensive overview of the challenges within geological modelling and visualization, which are widely relevant today and are still referenced in many papers. Of particular interest, he discusses the difficulties and differences in modeling different types of geological systems: "layer-cake" sedimentary environments, faulted environments and complex terrains – where layered sequences are not dominant, or complex geological structures are prevalent. In sedimentary environments, the stacks of sedimentary strata can fairly easily be modelled by creating individual stratigraphic surfaces. Additional inputs and methods must be used for the other two types of environments and the amount of expert user intervention increases.

The Mackenzie Plain is a sedimentary system, and through orogenesis in Late Cretaceous and Paleocene time, the geologic complexity has increased beyond the initial layer-cake type stratigraphy seen in other areas (Aitken and Cook, 1974). In addition, inputs available are not evenly distributed throughout the area, nor could they be considered dense. Consequently, the chosen methods will have to be slightly more complicated than those in a simple layer-cake stratigraphic model.

Solid modeling remains a popular method for modeling 3D geologic objects (Fisher and Wales, 1990; Lemon and Jones, 2003; Zhu et al., 2012). Lemon and Jones (2003) presented a fairly simple and intuitive technique of building 3D geologic solid models, which is still widely relevant today. Their approach, called the "Horizons Method", builds a model made up of geological horizons or strata, from boreholes and cross-sections. Most notably in their paper, they present a set of operations for representing common discontinuous geological phenomena (such as pinch-outs caused by the truncation of units at unconformities), which create problems when creating continuous surfaces from one that is discontinuous. These set operations allow us to automatically rectify the missing strata problem. It considers all potential types of missing strata, and therefore can control those features using only the boreholes.

A more recent, improved approach to the Horizons method and other methods that stemmed from it (Zhang et al., 2006) is the "Borehole-Surface-Solid method" developed by Zhu et al. (2012). This method considers the geological genesis of the

missing strata during the modelling, in order to properly model any discontinuities in the strata. They argue that their method has the potential for more automation and is more adaptable to a wider variety of geologic scenarios.

Most methods described here include boreholes as the primary input, as this is the case for the modelling in the Mackenzie Plain. However, building models from cross-sections, or using cross-sections to further constrain a model, has also proven effective (Lemon and Jones, 2003; Ross et al., 2005). However, Kaufmann and Martin (2008) point out that these models do not allow for easy updates should re-interpretation become necessary. The authors attempted to create a method that would allow for easier updating on models which was somewhat successful; however it still required a fair amount of expert user input.

The interpolation of individual surfaces, or the horizons, used to build up the solid model, is also a source of dispute. Namely, which interpolation technique is most appropriate to use is a matter of contention (Dag and Ozdemir, 2013). There exist almost countless methods possible or combination of methods. However, the most common methods are inverse distance weighting (IDW), triangulation and kriging (Caumon et al., 2009; Russell et al., 2011; MacCormack and Eyles, 2012). More recently, discrete smooth interpolators (Frank et al., 2007), polynomial methods (Dag and Ozdemir, 2013) or Bézier based techniques (Sprague and de Kemp, 2005), have been used. Each has its own set of merits. To further complicate matters, MacCormack and Eyles (2012) found that results can differ between apparently identical interpolation techniques, depending on the software program used.

The complexity of the 3D model and the set of operations as described in Lemon and Jones (2003), increase when discontinuities are present in the surfaces. For example, the presence of faults or unconformities, as seen in the Mackenzie Plain, can be problematic. Faults cannot be captured effectively with just boreholes. The authors do not present solutions to this, other than indicating they can be incorporated should the appropriate information be available and with additional steps. Wu et al. (2005) use the Horizons method and describes how to display faults using Delaunay triangulation and the mapped surface fault trace. Taking it a step further, if the horizons on either side of the discontinuity are displayed, one could model each surface on either side of the fault as if it was not present, and then cut the surfaces by each fault block, as suggested by

Caumon et al. (2009). The challenge with such a method is creating topologically correct intersections on either side of the fault and modelled surfaces (Turner, 2005). Wu and Xu (2003) describe and define all those potential topological spatial relationship problems and provide solutions to this problem.

Increased complexity in models also places more reliance and time commitments on expert individuals. Huang, Li and Han (2014) presented methods that would eliminate the requirement for human interaction with a model, and would still be able to effectively represent some more complex geological structures such as lens, pinch-outs, etc. However, their methods are limited to basic sedimentary environments where faulting and folding do not occur, which is not the case in the Mackenzie Plain.

Finally, as a result of continually evolving methods without strong standards, the accuracy of and/or uncertainties in the resulting models, are often questionable (Thorleifson and Berg, 2002). Given that the data being input into a model are often based upon subjective geologic interpretations and statistical interpolation/extrapolation techniques, most studies assess the model results in terms of "uncertainties" rather than "accuracies" (Tacher et al., 2005; Keefer and Rittenhouse, 2005; Lelliot et al., 2009). Lelliot et al. (2009) recognize that some studies simply visually assess the model results, whereas others attempt to quantity it. MacCormack (2010) uses a qualitative visual assessment and defines a "reliable" surface model. She defines it as one which "closely resembles the known stratigraphy and subsurface of the region, provides consistent results when repeatedly run, is compatible with information entered for individual data points, and is supported by data from 'proxy' sources". Proxy sources include indirect sources that can provide additional insight, or supporting evidence, to the 3D model. Perhaps one of the most simple depictions of uncertainty could be to create a color ramped layer of data density, as Keefer et al. (2011) created – higher data density signifying a lower uncertainty. Data density is only one of several factors influencing uncertainty however, and Lelliot et al. (2009) used data density, along with geological complexity, to provide an indication of uncertainty. Lelliot et al. also critiqued the statistical methods often used in most geoscientific uncertainty assessments, as they can fail to take into account the subjective nature of the data used in the model (i.e. the geologic interpretation), he presented an alternative, part qualitative assessment, to account for those issues. The quality of the input data can also negatively affect the accuracy of model outputs. In order to account for input

data with varying reliability, MacCormack (2010) presented a methodology for varying the influence data can have on a model output – higher quality data has a higher influence, and vice versa. Currently, there is no uncertainty or accuracy algorithm that can account for all types of uncertainties, though Wellmann et al. (2010) attempts to at least describe and provide a comprehensive classification of the different types.

2.2 Interpolation Methods Review

This section provides a general overview for the three methods of interpolation compared in this study. Readers should note that specific software programs allow for more or less control over input parameters. Therefore, results between software programs may, and have been shown, to vary slightly (MacCormack and Eyles, 2012). In addition, only brief descriptions of the algorithms are provided, and variations on each algorithm are possible. For more detail, readers can refer to any of the references cited.

2.2.1 Inverse Distance Weighting

One of the most common and easy to understand interpolation algorithms is inverse distance weighting (IDW) (MacCormack and Eyles, 2012). IDW is a deterministic interpolation method that quantitatively implements Tobler's first law on geography; that objects' characteristics are all related, but objects that are close together are more related than objects that are far apart (Tobler, 1970). Therefore, with IDW, when predicting a value of an unmeasured location, the known values closest to the unmeasured point will have a greater influence. A distance-weighting factor is applied to values within a specified search area. Close points are given more weight, and the exponent of that weight can be specified by the user, as well as the search area size and shape (Rockware, 2016). This type of interpolation is most suited towards datasets that are uniformly and/or densely distributed, as it is sensitive to clustering, as well as to outliers (Luo et al., 2008; ArcGIS, 2016; Rockware, 2016)

Due to its simplicity, it is widely used, and it has been proven to perform best in certain interpolation scenarios (Weber and Englund, 1992; Lu and Wong, 2008). However, in most geological research that uses IDW, the "correctness" of the geological surface is not the focus of the paper; rather it is upon a different methodology. For example, Lemon and Jones (2003) used IDW in their Horizons Method of modelling, but do not

touch on the effectiveness of this interpolation algorithm in visualizing geologic features.

2.2.2 Kriging

Kriging is a similar, but more advanced interpolation algorithm than IDW. It is based on the same idea of using known points and a distance-weighted algorithm to predict values at unknown points. However, unlike IDW, kriging is a stochastic algorithm that uses a semi-variogram to quantify the spatial autocorrelation between measured points as a function of the distance between them (Mallet, 2002). The semi-variogram is then used to determine the optimal weights. Consequently, it is known as being the best linear unbiased estimator. Kriging works well with large sample populations; as well, it can handle irregularly spaced data in certain circumstances (Rockware, 2016).

Zimmerman et al. (1999) compared kriging and IDW methods on several different types of mathematical surfaces and found that kriging methods out-performed IDW methods in all scenarios. However, the performance of the interpolation algorithm is highly dependent on the type, distribution of data, and above all, the surface that we are attempting to interpolate. Jean et al. (2004) used kriging methods to successfully model geologic surfaces (depositional facies). In contrast, Passey and Varming (2010) found that neither kriging nor IDW were able to produce acceptable results for creating lithohorizons. They found that they created bulls-eye type anomalies that were not consistent with the geological understanding of the region. Marinoni (2003) found that the smoothing in kriging, particularly around areas of no values (i.e. 0 thickness), is undesirable for most geological applications. However, by incorporating a probability criterion used in “indicator kriging”, he was able to yield more acceptable results. The author also states that the stochastic dependence, which is accounted for within kriging algorithms, could be attributed to geological processes such as sedimentation. Stephenson et al. (2003) also found that kriging performed poorly when dealing with discontinuous datasets, such as those commonly found within geological modelling, even with good data support. Still, kriging remains one of the most widely used interpolation methods in geology, and for interpolating surfaces from borehole data (Wu et al., 2005; Russell et al, 2015; Kis, 2016).

2.2.3 Triangulation (TIN surfaces)

This method creates surfaces by constructing triangles between control points and interpolating surface from locations on the triangular mesh. There are different methods of forming these triangles, however the premise of creating the triangulated surface from points or vertices, is the same. Resulting surfaces are often blocky in appearance (Zlatanova and Prosperi, 2006; Rockware, 2016).

There are fewer scientific studies done comparing different algorithm performances with one based on triangulation, at least in the geosciences. Nonetheless, the British Geological Survey, who have been at the forefront of advancing 3D geological modeling technologies since the beginning of their application, use triangulation methods in their own, in-house software package: GSI3D. Liu et al. (2015), have used triangulation to model 3D ore-bodies in the subsurface. Caumon et al. (2009) encourage the use of triangulation for several reasons, one being that it allows for spatially varying resolution on geologic surfaces, depending on the level of detail needed (e.g. more triangles created in high curvature areas, or areas with high data density). In addition, unnecessary nodes can be eliminated, or even densified to increase resolution in specific areas.

3.0 STUDY AREA

3.1 The Mackenzie Plain

The “Mackenzie Plain” is a region along the Mackenzie River drainage system, in the vicinity of the communities of Tulita and Norman Wells. This area is located in the western half of the Northwest Territories of Canada, just south of the Arctic Circle. The Mackenzie River runs from southeast to northwest through the region and empties into the Beaufort Sea. The river here is a broad and braided river. The Plain is bordered by the Mackenzie Mountains to the southwest and the Franklin Mountains to northeast (Figure 3.1). Between the two ranges is a forested, low-relief plain, blanketed by thin, unconsolidated Quaternary deposits with numerous small lakes (Government of Canada, 2011; Fallas et al., 2015).

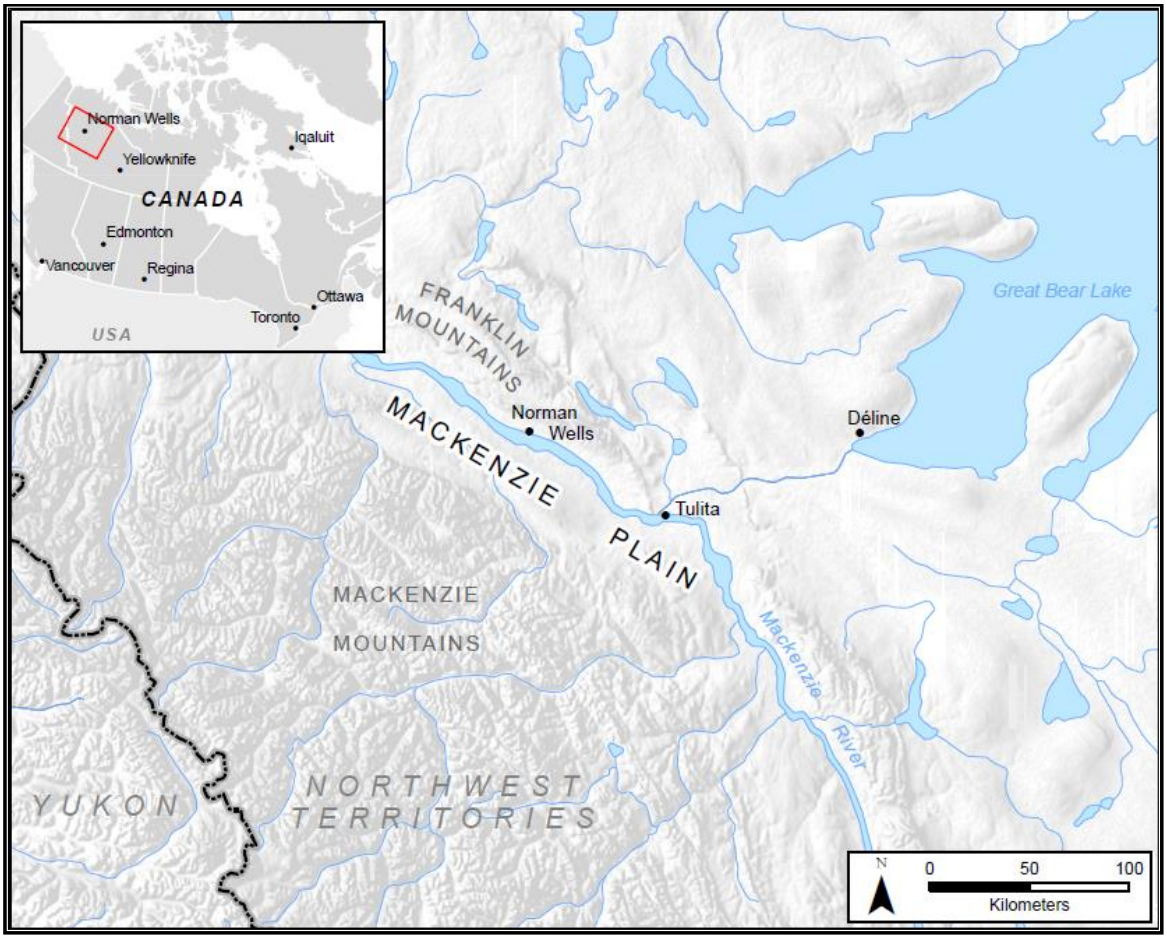

Figure 3.1. Mackenzie Plain and surrounding geographical area

3.1.1 Mackenzie Plain Subset

A portion of the Mackenzie Plain region was chosen for modelling. This subset was chosen because of the availability of well data and seismic survey sections in the region, attributable to recent petroleum exploration activities. As well, it exhibits several folds and a fault, for the testing of geologic structural visualization. This area is approximately a 2500 square kilometer area just south of the town of Norman Wells, with the Mackenzie River running diagonally across it (Figure 3.2).

The bounding UTM coordinates for the study area are (Zone 11N, NAD83):
Easting Max: 642,500
Easting Min: 591,500
Northing Max: 7,238,400
Northing Min: 7,189,500

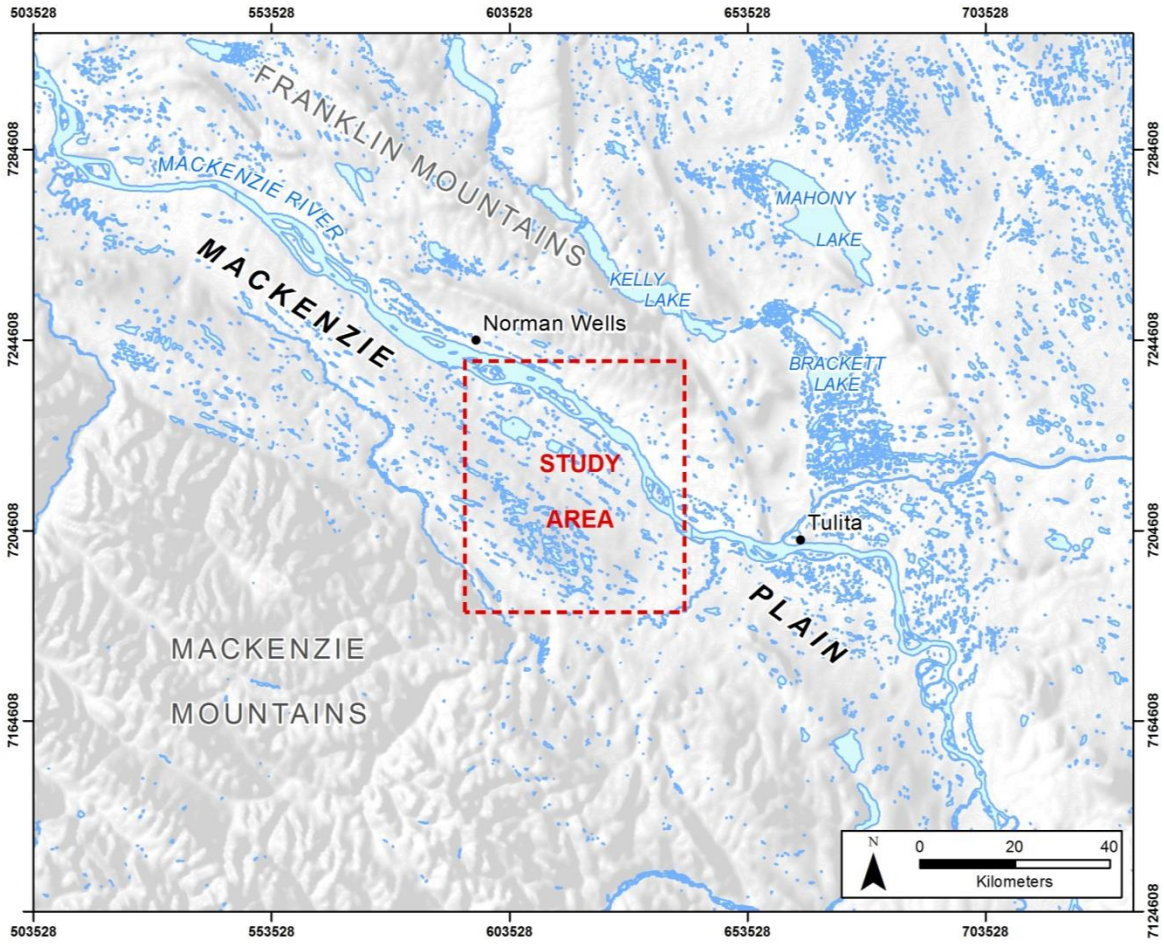

Figure 3.2. Study area within the Mackenzie Plain

This study area holds 19 wells, drilled between 1924 and 2012, as part of the on-going petroleum exploration in the region (Figure 3.3). The area is also covered fairly well, particularly in the north near Norman Wells, with 2D seismic survey lines.

Folding in the area is exemplified by the Loon Creek anticline, Mirror Lake anticline and Twentyfive Mile Lake syncline, in addition to several small monoclines. A thrust fault is also visible in the southwest corner of this area, in the front ranges of the Mackenzie Mountains (Figure 3.3). This allows for testing of methodologies in areas with non-horizontal layering and discontinuities.

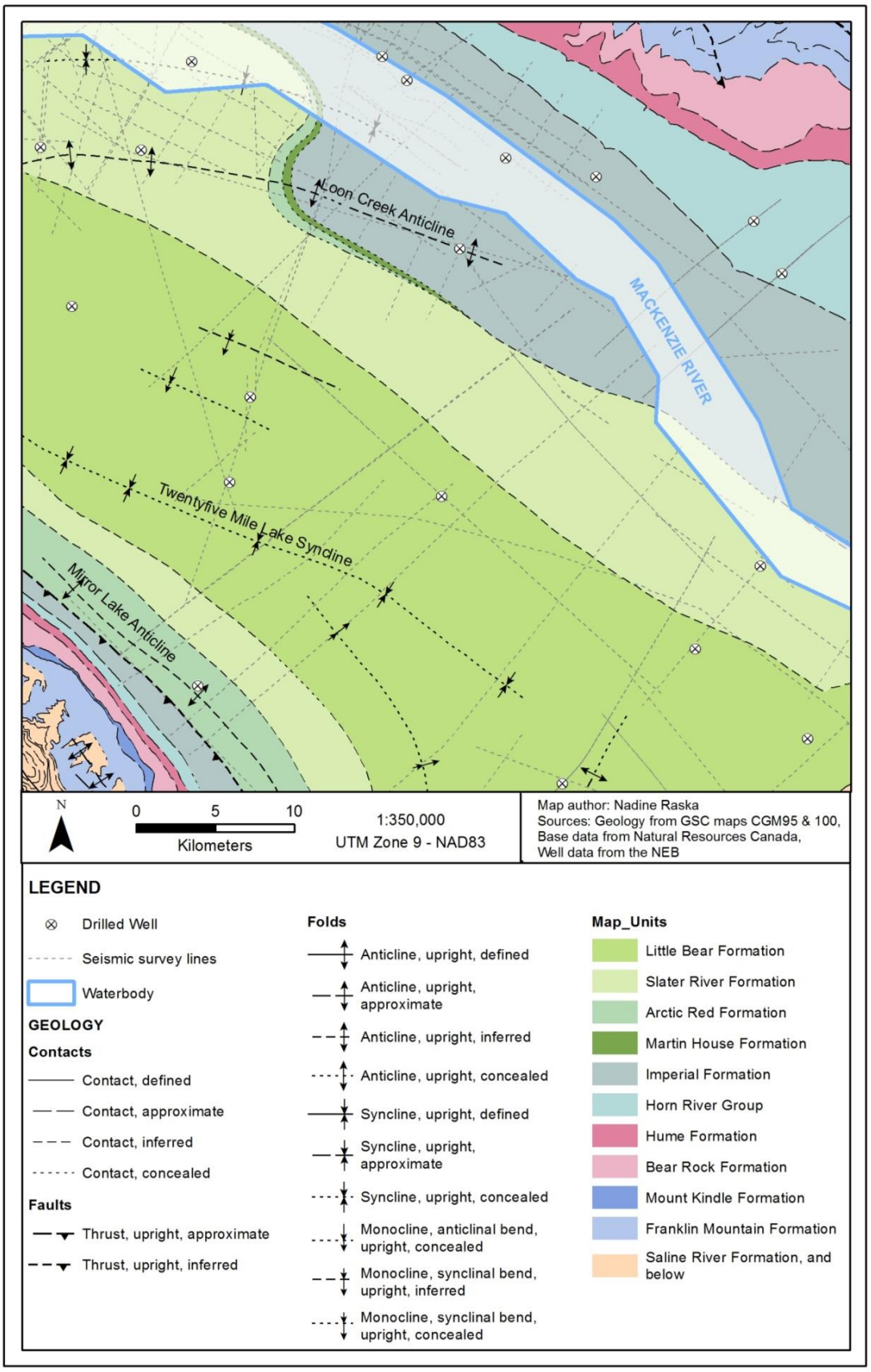

Figure 3.3 Map of geology and seismic survey lines

3.2 Geologic Setting

The Mackenzie Plain is situated in the northern part of the Western Canada Sedimentary Basin (WCSB) – a massive wedge of sedimentary deposits more than 6 km thick in sections, underlying 1 400 000 km² of Western Canada. The WCSB extends from the Rocky Mountains and Mackenzie Mountains in the West (the Cordilleran foreland fold and thrust belt) to the Canadian Shield in the east, and has one of the world's largest reserves of petroleum and natural gas (Mossop and Shetsen, 1994; Fallas et al., 2015; Natural Resources Canada, 2016). In a simple sedimentary basin we would find chronological, vertical stacking of horizontal sedimentary strata. This is the type of system where the "layer-cake" description of sedimentary strata was conceived. In a more complex system, unit boundaries can be broken by discontinuities such as faults, unconformities or other geological features (Popovs et al., 2015).

The mountain ranges surrounding the Mackenzie Plain were created in the Late Cretaceous through Paleocene (between 100 million years ago and 55 million years ago; Powell et al., 2016). Compressional tectonics has shaped this region, causing the uplift and deformation of sedimentary rocks adjacent to and within the Mackenzie Plain. This resulted in long wavelength folds, bedding parallel detachments, and thrust faults which outcrop in the Mackenzie and Franklin Mountains (Williams, 1990). The basin thickness in this region is over 5 km in the foothills belt, and shallows towards the east (Natural Resources Canada, 2016).

Due to limited bedrock exposure in areas of the Mackenzie Plains, geologic interpretation for bedrock mapping has been augmented by interpretation of reflection seismic lines, predominantly acquired by industry, and available to the public via government institutions (Cook and MacLean, 2004). For more detailed information on the bedrock geology, readers can refer to the published Canadian Geoscience Maps: CGM 95 (Carcajou Canyon, northeast), CGM 100 (Norman Wells, southeast), CGM91 (Mahony Lake, southwest) and CGM92 (Fort Norman, northwest) (Fallas and McNaughton, 2013; Fallas et al. 2013a, Fallas et al. 2013b, Fallas et al. 2013c). The maps were generated at a scale of 1:100 000 and delineate the bedrock geology at the surface, as well as the geologic structures. They can be found online through the Natural Resources Canada geoscience search portal: Geogratis (www.geogratis.gc.ca)

Note that for the purposes of this study, some formations have been grouped. These will be described further in a following section.

4.0 DATA

All inputs to this study are publicly available datasets, produced by either government, or industry. The primary inputs to the modeling process and to the creation of the stratigraphic surfaces were the stratigraphic unit contacts at the surface, and the stratigraphic contact picks in the subsurface. Additional data was used to guide knowledge on what the subsurface should look like, and to help constrain the models where the primary inputs were not available.

4.1 Wells

The primary dataset used for modeling the subsurface were well logs, also referred to as boreholes in this paper. This is the only true sampled information from the subsurface. Information provided by this data includes operational information of the well, logs, test results and geological descriptions of samples. For this study, the relevant information includes the well locational information and subsurface stratigraphic contact depths, or picks, which are provided by a top and a bottom depth. These picks form the basis of the points used in the stratigraphic surface interpolation. Depths are stored as below surface depths. That is, 0 means at the ground surface, and 100 meters denotes 100 metres below the ground surface.

There were 19 wells that are located within the study area. Well logs can be obtained through the Frontier Information Office of the National Energy Board (NEB) by request (NEB, 2016).

4.2 Bedrock Geology

The surface bedrock geologic data was published as part of the Canadian Geoscience Map series (CGM) at a scale of 1:100 000. Both the maps and digital GIS data can be downloaded by the public from Geogratis (www.geogratis.gc.ca). Data is available as shapefiles, an ArcGIS compatible format, and a description of the contents and its metadata are included in the download.

The study area crosses two CGM maps: CGM 95 (Carcajou Canyon, northeast) and CGM 100 (Norman Wells, southeast). The following datasets from the published CGM data were used:

Contacts – Line features that show the location of contacts between stratigraphic map units, where they intersect surface topography. These are simply line features that do not provide information about the units on either side of the contact. For that information, the user must refer to the map unit polygons.

Map Units – Polygon features that show the extent and type of stratigraphic map unit at the surface. A description of the map unit is also provided here.

Faults – Line features that represent fault traces, shear traces, or structural lineaments. Applicable information contained within the fault attributes includes the type (e.g. thrust), the attitude (e.g. upright or overturned), and the hanging wall side, if applicable, of the fault. This gives users the basic knowledge on the orientation of the fault beneath the surface, but does not provide specific measurements.

Folds – Line features that show fold traces. Applicable information contained within the fold attributes includes the type of fold (e.g. anticline, syncline), the attitude of the limbs (e.g. upright or overturned) and the trend and the plunge of the fold axis. Again, this gives user the basic knowledge on the orientation of the fold in the subsurface, but not numerical measurements.

Measured Sections – These sections characterise the thickness of different stratigraphic units and their relationships to each other. This gives users an estimate of the thickness of the unit in a particular area. Downloaded data is provided as a line shapefile of the path of the measured section, and provides information in the attributes on where the measured section information is published, so that users can locate it for more detailed information.

Planar Measurements – Point features that represent an orientation (strike/dip) measurement. This information was used in the qualitative assessment of the model as it provides us information on which direction the stratigraphic layers are dipping.

More geologic information is provided in the download, however for the purpose of this study, this supplementary information was not used.

Data was projected into UTM Zone 9N, NAD83, and clipped to the study area.

4.3 Reflection Seismic Data

The Mackenzie Plain area has reflection seismic survey coverage due to oil and gas exploration in the region. Some reflection seismic profiles collected by industry have been made available to the public, and are archived with the NEB, again available through the Frontier Information Office (NEB, 2016). Processed data images show the subsurface in two-way time versus distance along the seismic line and the position of the reflectors must be converted to depth. Two-way time is the travel time from the surface, to the reflector in the subsurface, and back. To perform the conversion, the speed at which a sonic wave passes through different rock types must be known, as well as the rock types present. These properties were determined by integrating well and seismic data as described in MacLean (2011). Data used in this modelling study was extracted from MacLean (2012).

This seismic data helps constrain the location and style of structures, particularly in areas with no well data. Analyzing and converting structure orientations and stratigraphic map units in the seismic profiles is time consuming and requires expert interpretation, however they may still be used for a qualitative assessment to view the approximate orientation of the structures in the subsurface.

Interpreted seismic data was available in the form of depth-to contours (the conversion from time already performed), with a height datum of 305 meters above sea level. Therefore, it was necessary to convert their heights into a depth from surface measurement. This was done by subtracting the measured contour depth from 305 meters, to obtain a depth above sea level for a particular horizon, and then by adding the DEM height, to obtain a depth below surface (Figure 4.1).

The contours were then converted to a raster format, in ArcGIS. First, a TIN was created from the contour lines, and this was then converted into an ESRI GRID file. This was done because the ESRI Grid files are easily read by the geomodelling software, Rockworks17.

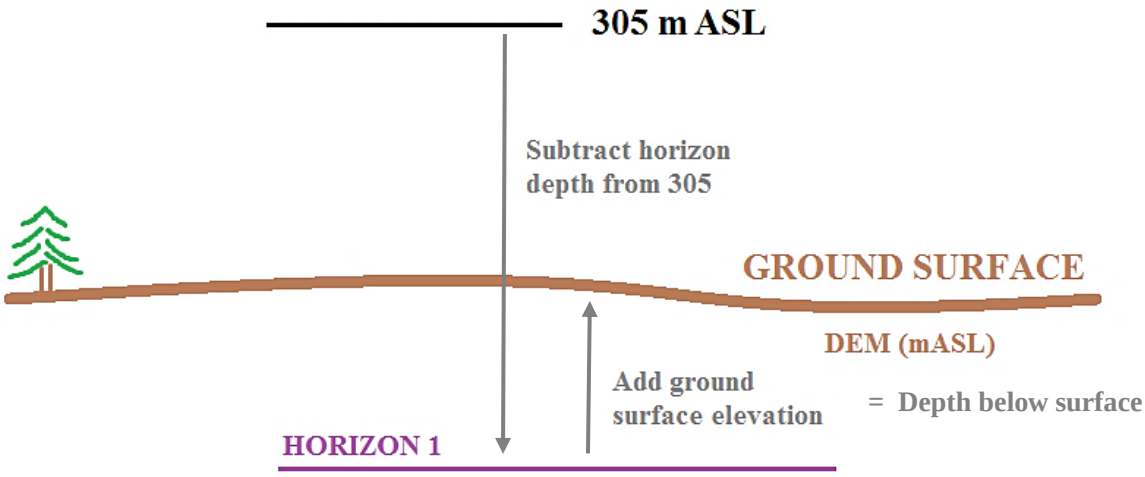

Figure 4.1 Schematic of determining surface stratigraphic depths in depth below surface

4.4 Digital Elevation Model

Produced by Natural Resources Canada, and called the Canadian Digital Elevation Model (CDEM), it represents elevations as measured at ground level. These elevations are interpreted via stereoscopy, digitized contour data, GPS data, or radar (Government of Canada, 2014). It is downloadable by the public from the Geogratis website (see above). The study area covers parts of 4 NTS map sheets, namely 96C, 96D, 96E and 96F. The data is supplied in TIFF format with a pixel size of approximately 15m. More information on the creation of the dataset can be found online and with the metadata supplied when downloaded.

The 3 NTS map sheet DEMs were mosaicked into a single GeoTIFF file and projected into UTM Zone 9N, NAD83. They were then clipped to a shapefile of the study area footprint.

4.5 Ancillary Base Map Data

Additional base map data used for mapping purposes is from Natural Resources Canada CanVec digital cartographical reference product. This data is also downloadable via Geogratis as shapefiles.

5.0 METHODS

There are three main steps, which are generally universally present in a 3D geological modelling workflow. They are data compilation and preparation, the 3D modelling process, and results analysis / accuracy assessment (Caumon et al., 2009; Kauffman and Martin, 2008; Matile et al., 2011; Turner, 2006). This general workflow for the geological modelling process can be seen in Figure 5.1.

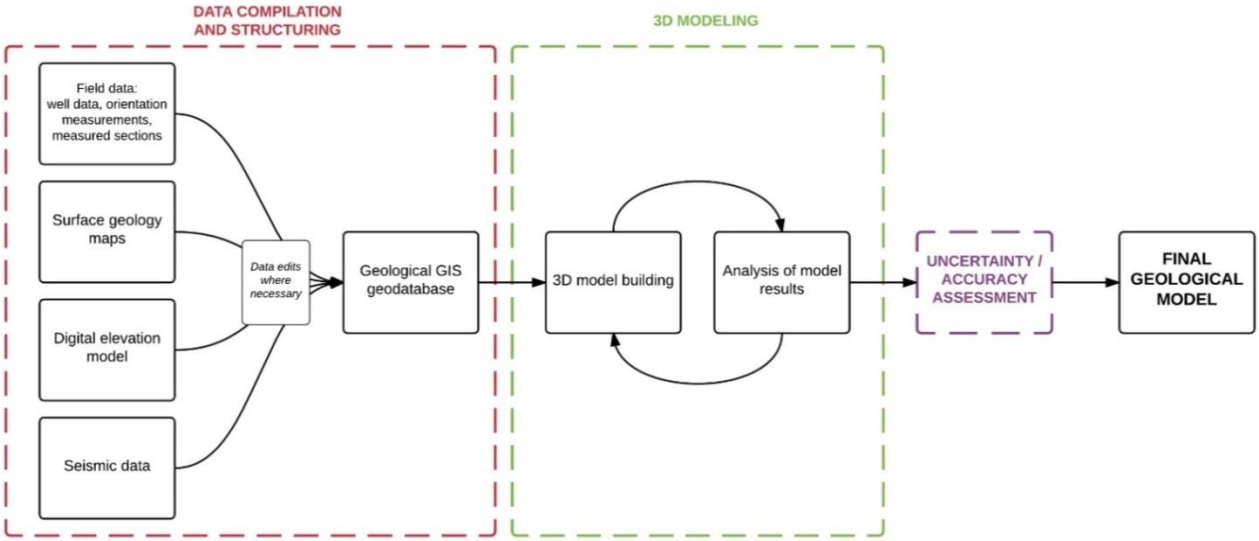

Figure 5.1. General geological 3D modelling workflow

Depending on the input data types used, the data compilation stage can be done within any database or any software capable of GIS visualization. For the 3D modelling process, geomodelling software, capable of visualizing in 3D, is necessary. The method chosen here could be implemented in many different types of software programs.

5.1 Software Considerations

In this study, spatial GIS data was stored in an ArcGIS file geodatabase. Additional attributes such as well information was stored in an Excel file and linked to the spatial point features.

An appropriate 3D interpolation method and visualization package must be used for the modelling process. Criteria used for determining the software to be selected are based on not only software capabilities, but resources as well. This includes financial

resources, in addition to computational resources. This is not an inconsequential step, as needs and available resources do not always match up (Turner, 2006). For this study, Rockware's Rockworks17 was used as the geomodelling software, and ESRI ArcGIS 10.2 was used for any other spatial data processing tasks. The Rockworks software was chosen for the geomodelling for several reasons, including the intuitive layout, the ease of creating simple cross-sections and, particularly, the ease of converting data between different file formats (e.g. from Rockworks grid files into ArcGIS shape or grid files).

5.2 Horizons Method

The chosen methodology for the 3D modeling follows one introduced previously, developed by Lemon and Jones (2003), called the Horizons Method. The Horizons Method was developed by Lemon and Jones as a methodology for creating 3D geologic models in sedimentary systems, from boreholes. It essentially models the top and bottom surfaces of a formation, and using a set of rules, combines them into one cohesive subsurface model. This methodology was chosen for this study because of its simple, intuitive nature, and the flexibility of the set of operations described for dealing with discontinuous geological phenomena, which occur in the Mackenzie Plain. The bottom to top modeling approach is conducive towards sedimentary environments, as it follows the sequential order in which sediments are deposited. In addition, this approach can be modified and used in almost any software program capable of interpolating raster surfaces.

A brief description of the methodology is as follows:

Step 1: Assign Horizon IDs to boreholes – A value is assigned to the top elevation of each horizon in the boreholes, in a bottom to top depositional sequence. Accordingly, the top of the lowest modelled geologic unit will be 1, and the ID will increase moving upwards to the more recently deposited units.

Step 2: Define a primary TIN – A triangulation interpolation algorithm is to be used to define the outer boundary of the modelled volume. This also establishes the topology for all the interpolated horizons to ensure topological consistency throughout the model when horizons are intersected.

Step 3: Interpolate horizon elevations – Horizon elevations from the borehole horizon IDs must be interpolated, and surfaces created, using any interpolation algorithm desired. This creates an elevation surface for each horizon ID, or stratigraphic unit.

Step 4: Intersect horizon surfaces – The surfaces of each horizon are intersected with each other, starting at the bottom with the oldest units. The primary TIN is modified so that it contains all points from all possible intersections.

Step 5: Adjust horizon elevations – No elevation of any given surface can extend below the elevation of the surface underneath it. Starting again from the bottom up, if the elevation of the horizon above the one in question extends below it, its elevation is set to be equal to the one under investigation.

Step 6: Build solids – Horizon elevation surfaces are extruded and the solid model created. Since all possible intersections have been previously defined, there will be no voids or overlapping solids.

For a more detailed description and analysis of this method, readers can refer to the paper by Lemon and Jones (2003). The Horizons Method covers mainly the "3D modelling" step of the typical 3D geologic modelling workflows, however the setup of the horizons can be considered to be part of the data compilation and preparation stage.

For this study, we will assume the "horizons" referred to by Lemon and Jones, are stratigraphic units. These units are composed of the same or similar materials, are of a fixed depositional age range, and consequently they exhibit similar properties and can be considered a coherent rock mass (Turner, 2006; Zhu et al. 2012).

5.3 3D Modelling Methods

5.3.1 Data Preparation / Compilation Stage

5.3.1.1 Project Set up

The parameters for the modelling had to be defined at the beginning. The extent of the study area was as described in Section 3.0: Study Area. The model, in terms of 3D space and resolution, also had to be defined. The XY resolution, or node spacing, was set to 250 meters, and the Z resolution set to 25 meters. This resolution may appear to be low with such a large cell size, however the area being modelled is relatively large. In

addition, a smaller cell size drastically increases processing time, so for an iterative process such as in this study, quick re-processing of surfaces was given more importance than increasing the level of detail in the sparsely constrained model. A Z resolution of 25 meters was found to produce aesthetically reasonable results, while allowing for the quick reprocessing of surfaces. Every surface will use this node structure and extent as its spatial structure/boundary.

The coordinate system of the project was set to be UTM Zone 9N, North American Datum 1983.

5.3.1.2 Data Compilation

Geological data can exist in many different forms, from many different sources. Data can be in digital or hardcopy format requiring digitization, and come from either industry or government sources, with varying collection methods and standards. Particularly in frontier regions such as the Mackenzie Plain, where the geology had been previously mapped in the mid-twentieth century (and only since more recent interest was shown due to oil and gas exploration), is the area being revisited (Dixon et al., 2007; Fallas et al., 2015). Data in these regions often exist as historical bedrock field observations or hardcopy maps, and may not be available in a digital format. More recent and more detailed information, particularly reflection seismic data, may be held privately by industry and often are not available to the public or government organizations. Each project may require, or have access to different data sources and experience difficulties at difference stages of the compilation process.

The data used in this study can be found in Section 4.0 – Data.

All the input data must be compiled, assessed for completeness, and updated as necessary. Some data may exist in different projections, or the geological interpretation might be inconsistent between different sources. This could be due to the scale at which they were first mapped or the geological state of knowledge at the time of interpretation (Kaufmann and Martin, 2008). The geological data must also be stored in a database in a rational data structure, which retains the relevant geological data attributes and is compatible with the modelling process. Accordingly, data must be organized, reconciled, and put into an appropriate spatial, digital format. This step, although often tedious and time-consuming, is crucial for effective modelling (Kaufmann and Martin,

2008). Data must also be organized according to the specifications of the Horizons methodology.

5.3.1.3 Database Structure

The most appropriate organizational structure of datasets will depend greatly on software used. Geologic features from published maps in this study were stored as feature classes within a feature dataset in a file geodatabase. Stratigraphic unit depth grids, from the seismic surveys, as well as the DEM, were stored as rasters within the geodatabase.

Well data was stored as both a feature class, and a related Excel worksheet. Wells were stored as points, which represented the location of the wells within the study area – their locations will not change with updates, but new well locations can be added. Information about stratigraphic unit depths was stored within an Excel worksheet. The Excel worksheet can be joined to the GIS feature class based on a unique well identifier (UWI) code, with a one-to-many relationship. There can be multiple entries for each stratigraphic surface depth, but only one for each well (Figure 5.2). This type of structure allows the database to be normalized and it is also the format in which the used geomodelling software (Rockworks17) organizes its well/borehole data.

1

UWI	Easting	Northing	Elevation	TotalDepth
300A376500126000	637168.60	7204336.40	126.49	3000.00
300A496500125450	647217.31	7208835.23	111.00	3000.00
300A526520126450	597943.83	7230701.90	105.71	3000.00
300B146520126300	614789.11	7235112.30	60.61	3000.00
300B256520126300	613201.61	7236620.39	63.29	3000.00

∞

UWI	TopDepth	BottomDepth	Stratigraphy
300A376500126000	0	157	SLATER RIVER FM
300A376500126000	157	662.9	IMPERIAL FM
300A376500126000	662.9	862.3	HORN RIVER GP
300A376500126000	862.3	996.7	HUME FM
300A376500126000	996.7	1336.7	BEAR ROCK FM
300A376500126000	1336.7	1616.7	FRANKLIN MOUNTAIN
300A376500126000	1616.7	3000	SALINE AND BELOW

Figure 5.2 Schematic of borehole location data and joined Excel table

5.3.1.4 Data Reconciliation / Completion

It was necessary to ensure that all stratigraphic unit groupings and specifications were consistent. In some wells, units were grouped or undivided, likely due to limited knowledge at the time of drilling. Or, if the original drillers were only interested in locating certain oil-bearing formations, they would group certain units into age groups (e.g. Cretaceous). Consequently, a stratigraphic lexicon of the desired units to be modelled was created and the well data updated (Table 5.1). In addition, certain older units were grouped, as there were not enough wells that penetrated to that depth, nor other geologic information that could be used to estimate their thickness. At this stage, we also assigned horizon IDs that corresponded to the borehole unit contacts.

Table 5.1. Stratigraphic lexicon and corresponding horizon IDs

Units Present in Wells	Units/Horizons for this study	Horizon ID
Little Bear Formation	Little Bear Formation	1
Slater River Formation	Slater River Formation	2
Arctic Red Formation	Arctic Red Formation	3
Martin House Formation	Martin House Formation	4
Imperial Formation Canyon Member	Imperial River Formation	5
Canol Formation Kee Scarp Fm Ramparts Formation Hare Indian Formation Bluefish Member	Horn River Group	6
Hume Formation Nahanni Formation Headless Formation	Hume Formation	7
Landry Formation Bear Rock Formation Arnica Formation Fort Norman Formation	Bear Rock Formation	8
Mount Kindle Formation	Mount Kindle Formation	9
Franklin Mountain Formation	Franklin Mountain Formation	10
Saline River Formation Mount Cap Formation Mount Clarke Formation	Saline River and Below Formations	11

Next, it was necessary to ensure there were no incomplete wells, and that any missing formations represented real geological features and were not simply omissions in the reporting. This step required the knowledge of an experienced geologist, as it this was determined by looking at various regional geologic factors. For continuity when creating a continuous surface, it is necessary for the complete stratigraphic profile to be present at each well, particularly when there are only a few wells to begin with. There

were two scenarios that would result in a formation missing from a well, and they were dealt with separately.

1) Unit pinches out - If a unit was not present due to it pinching out, it was assigned a thickness of 0 by setting the top and bottom depth to be the same value, as shown in Table 5.2.
2) Drilling stopped – If the unit was not present because the well did not reach its depth, but it was present below, it was necessary to extrapolate those depths, or total unit thickness. The specific methods are described in the next section.

Table 5.2 Example of well (UWI: 300C176510126000) with a depth of 0 for Mount Kindle formation

Depth to Top (m)	Depth to Base (m)	Formation
0	146	HORN RIVER GP
146	227.1	HUME FM
227.1	565	BEAR ROCK FM
565	**565**	**MOUNT KINDLE FM**
565	869.6	FRANKLIN MOUNTAIN
869.6		SALINE AND BELOW

Finally, to ensure elevations from the wells and the downloaded DEM matched, well elevations were updated to correspond to those measured from the DEM. The DEM surface elevations were considered to be the most up to date as it was created more recently than some of the drilled wells. The formation elevations below were also updated to reflect this change.

5.3.1.5 Unit Thickness Estimation

Thicknesses were estimated to complete boreholes that did not have the entire stratigraphic profile described. For instance, if there was only a top elevation at the bottom of a well, but no base elevation of a unit, this was problematic. Estimating the thickness of a unit allows us to calculate either the top of bottom subsurface elevation of a unit.

In the data available, there was a depth measurement down to, at minimum, the top of the Hume Formation in 15 of the 19 wells. Due to the reliability and confidence in the

seismic surface depth of the Hume Formation (as it is has an obvious seismic signature), it was possible to extract a depth at those four wells that were missing depths below the Hume formation top. For the older units at deeper depths, the seismic depth estimates were not as reliable, for various reasons. Therefore, it was necessary to make assumptions on the thickness of those units, using the geological data available and current scientific understanding of the subsurface stratigraphy.

Based on reflection seismic images across the Mackenzie Plain showing gradual thickness changes for each of the units above the Saline River Formation, it is generally possible to assume that if there are no abrupt disruptions, such as faults, thicknesses will vary smoothly from thinner to thicker areas. This allows for some predictability in unit thicknesses in areas where direct measurements are not available. For example, the Hume Formation has a fairly consistent thickness across the study area in the wells in which the full thickness was present. Therefore, where a bottom depth of the Hume Formation was not provided, its average thickness was used to extrapolate downward from the top of the unit.

Determining the bottom of the Hume Formation also gave us the top of the Bear Rock Formation. This unit varied slightly more in its thickness across the region, therefore its thickness was determined by taking an average of the two closest wells. This way it was not influenced by wells far away, as it would be if an average thickness across the whole area were used.

The bottom of the Bear Rock Formation established the top of the Mount Kindle Formation. However, of the six wells drilled through the Mount Kindle interval, a thickness greater than zero was measured in only one well, that closest to the Mackenzie Mountains. Measured thicknesses in the Mackenzie Mountains (Pope and Leslie, 2013) and the nearby well show that the Mount Kindle Formation is present in the southwest corner of the study area, and the other five wells indicate that the unit pinches out towards the northeast.

Finally, the top of the Franklin Mountain formation was either the bottom of Mount Kindle, or Bear Rock, depending on if Mount Kindle was present or not. Once again, the thickness of this unit was based on measured thicknesses in nearby mountain exposures, and sparse well control. From the well penetrations and seismic evidence, the unit is thickest in the southwest corner and gradually thins to the northeast.

A summary schematic of the process is illustrated in Figure 5.3 and is further described in Section 6.1.1: Data Compilation and Derived Thickness Estimates.

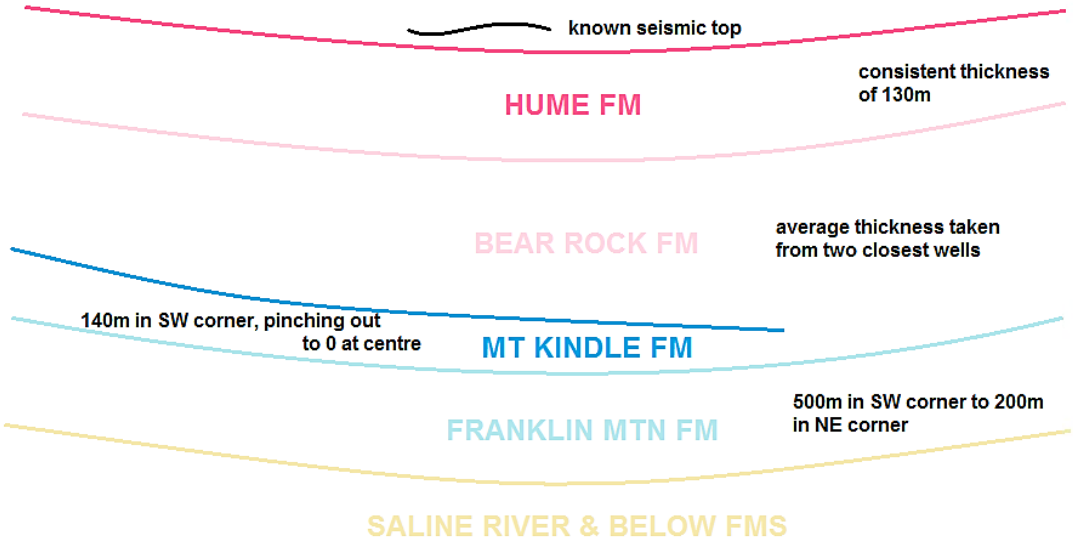

Figure 5. 3 Process of estimating formation thicknesses / depths in wells

5.3.1.6 Additional Control Points

Using only the 19 boreholes/wells, over a 2500 km² area, there is not enough control to create realistic geological surfaces over such a large area with folded strata. As there is a major syncline passing through the study area, older units are being forced up to the surface at the edges of the study area, and the location of those contacts at the surface are not effectively captured by the borehole data alone. Therefore, it was necessary to incorporate the surface contacts at this stage as well. This was done by creating "ghost" wells, which are used in the same manner as the regular wells in the interpolation process. These points were created at 3 km intervals along the mapped contact line, in ArcGIS, creating a total of 170 points. At these points, the unit that reached the surface is assigned a top depth of 0, which is equivalent to the surface elevation, extracted from the DEM. This allows the interpolation algorithm to incorporate the information that the unit being interpolated came up to the surface at that location (Table 5.3).

Table 5.3. Example of ghost well

Depth to Top	Depth to Base	Formation
	0	Little Bear Formation
0		Slater River Formation

In addition, three additional wells were created in order to properly model the faulted area in the southwest corner, and are described in section 5.3.2.5: Faults.

Adding additional control points such as these are necessary in order to construct geologically correct surfaces in areas of more complex geology and/or missing strata (Lemon and Jones, 2003; Wu et al., 2015).

5.3.2 3D Modelling Stage

Once all the stratigraphic data was validated and complete, the construction of the three-dimensional model begins. The workflow for creating the 3D model roughly followed the Horizons Method as developed by Lemon and Jones (2003). Slight deviations from the Horizons Method were necessary to account for the types and availability of data for this specific project area, as well as software program intricacies.

The first two steps of the Horizons Method, assigning horizon ID's and defining an outer boundary, were performed in the data compilation/project set up stage.

5.3.2.1 Horizon / Stratigraphic Surface Interpolation

The next step was to interpolate the individual stratigraphic surfaces from the downhole well data. This step was performed in Rockworks17. Three different interpolation algorithms were used and the results compared, specifically IDW, kriging, and triangulation. These three were chosen as they are three of the most commonly used interpolation algorithms, and the intention was to determine how well suited they are to producing interpolated geological surfaces (Caumon et al., 2009; Russell et al., 2011).

The software program used in this study allows for several parameters in the IDW algorithm to be set. Namely the weighting exponent, the number of points included, and a sector search angle. The weighting exponent determines the weight of nearby points versus far, and a lower weighting exponent results in a more localized

interpolation. The number of neighbours determines how many points are used in the interpolation (Rockware, 2016). Different numbers were tested for each of these parameters and the results assessed. The sector search angle was kept circular, as there was no indication of any directional bias.

As with IDW, there are several parameters that can be changed within the kriging interpolation algorithm, specifying the variogram options as well as the number of neighbours. The variography was set to automatic, so that the software program would compute the optimal model to be used. However, several numbers of neighbours were tested. The number of neighbours indicates how many data points will be used, and the higher the number, the more regional influence we see in the resulting interpolation (Rockware, 2016).

A smoothing filter was also applied after the interpolation for each stratigraphic surface to ensure a smooth surface. Without the presence of any faulting or other discontinuity, geologic surfaces should generally be smooth as can be seen within the seismic images in this study area. A 3-cell smoothing filter was run, with three iterations. Rockworks also provides a "high fidelity" option in the interpolation process, which ensures the model honours the location of the control points, irrespective of any smoothing applied. This option was also applied, as honouring values at the known data points is very important.

Once the most suitable interpolation algorithm was determined, surfaces were interpolated for each stratigraphic unit, using that interpolation algorithm. The process used for determining suitability is described in Section 5.3.3: Results Assessment. Any unit that outcropped at the surface (in this case, all units except for the Saline River formation) was clipped to the DEM surface. This was done to ensure no surfaces were projected beyond the ground surface, which is possible depending on the interpolation algorithm used, or the accuracy of the surface elevations provided in the well data.

5.3.2.2 Overlapping Surfaces

Ideally, there should be little overlap between stratigraphic surfaces. However, this is difficult to accomplish when interpolating layers independently, particularly when large gaps between data points are common.

As per the Horizons Method, horizon elevations of individual stratigraphic surfaces must be adjusted where they extend below the unit below, or a gap is present. To ensure no small sliver gaps or overlaps were present even when not visible, the bottom surface of all units was set to equal the top of the surface below them. Starting from the oldest, bottom stratigraphic surface first, the surfaces were intersected and the model built from the bottom up.

For example,

Top of Saline River Formation = Bottom of Franklin River Formation

We do this for each gridded formation surface until we reach the youngest one, at the ground surface. The DEM is then used to clip, or to truncate, any unit that appears at the surface.

5.3.2.3 Manual Edits

Depending on the result of the modelled individual surfaces/horizons (described in the Results section), it may still be necessary to perform manual edits. This occurs when a surface does not conform to accepted geological principles, or does not appear as one would expect or as published elsewhere in the literature. The two scenarios in which manual edits were required are: If the unit does not pinch out in a manner or location we would expect it to, or when the unit extends out beyond the contact at the surface, referred to here as "bleeding" (Figure 5.4). These scenarios can be particularly prevalent in units that are discontinuous across the study area, or are very thin units. Modelling thin sedimentary units pose additional problems that are difficult to rectify without manual intervention (Tremblay et al., 2013). The Horizons Method does not provide guidance on steps for when manual edits are necessary to create a realistic model.

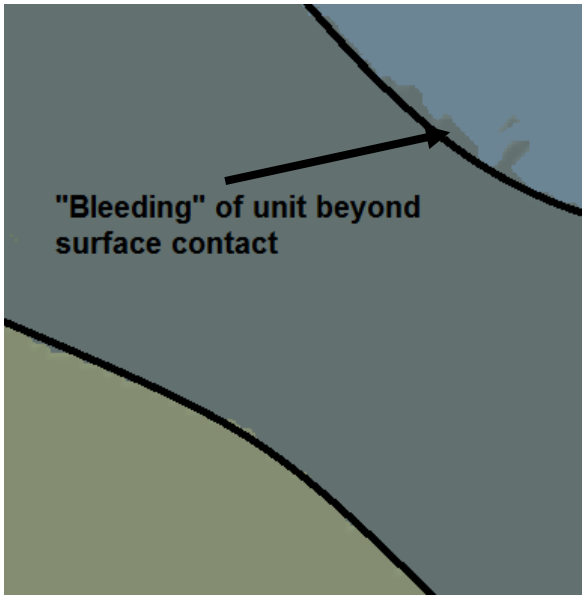

Figure 5.4. Unit pinching out below surface/bleeding.

Manual edits are performed on unit thickness values rather than elevation surfaces, as the thickness values are conceptually easier to edit than elevation values. Accordingly, individual unit thicknesses, as modelled, are calculated by subtracting the top and bottom of that unit:

Unit_Top – Unit_Base = Unit_Thickness

Next, the thickness values of the resulting grid are manually edited. Unit thicknesses are used in lieu of elevations as they are easier to edit and quantify what a reasonable thickness value would be, based of geological knowledge. Rockworks17 provides a "grid editor" where cells in a grid can be directly changed and values smoothed, or graduated. Changing values on a cell-by-cell basis would be extremely time consuming. Therefore, where manual edits were necessary, the following steps were performed:

To edit the extent of a unit, for example the limit of a unit pinching out, a polygon denoting the extent of the unit is drawn, representing a best estimate of the pinch-out, and all cells falling outside the polygon are given a value of 0. If necessary (i.e. the unit was quite thick on the inside of the polygon), a smoothing filter was applied to the edge cells, ensuring a smooth transition to 0. This gives us an updated unit thickness grid. This clip by polygon function is found within the Rockworks program, however it could also be done several ways within, for example, ArcMap via the Raster Calculator.

Next, to determine the new value of the bottom of the unit (*Unit_Base*), this new thickness grid must be subtracted from the top of the unit (*Unit_Top*). This *Unit_Base* is also set to be the top of the older unit below, to ensure no gaps were present.

Unit_Top – Unit_Thickness = Unit_Base (and underlying formation Unit_Top)

Where the thickness value was set to 0, the unit will not be visible and the top of the unit below the one in question will be coincident with the bottom of the unit above. If it is the outcropped formation at the surface whose contact needs proper delineation, the same process applies. The mapped contact lines are used to create a polygon of where the formation exists, and the thickness set to 0 beyond the polygon.

Manual edits were performed sparingly, and with caution, as there is little quantitative, defendable reasoning behind the changes. The changes are based purely on user intervention and are performed freehand. However, in order to have a geologically reasonable, aesthetic model, this step was necessary.

5.3.2.4 Building the Final Model

Once the individual stratigraphic elevation surfaces were satisfactory, the surfaces were extruded and a solid model was created.

Each formation surface top is extruded down to the formation base, which is also the top surface of the older formation below it. This is the case unless the unit has pinched out, in which case the bottom surface may fall on top of different formation tops, depending on their location.

In this study, a voxel model was used as the solid model, as this is the preferred method in Rockworks17. Voxel models are three-dimensional cells, or "volumetric pixels", attributed with a value or geological property, which define the entire study area. They are a common type of model in 3D geologic solid modelling (Flemming et al. 2013; Hoyer et al. 2015). It is possible to either create a voxel model directly, or convert gridded surfaces to a voxel model by way of extrusion of surfaces. The latter method was performed here.

5.3.2.5 Faults

Faults present a barrier in the otherwise continuous surface and are one of the most difficult structures to display in a 3D geologic model (Wu et al., 2015). The

stratigraphic surfaces may slide along a fault plane and create an abrupt displacement, which is not easily modeled via boreholes only.

In order to solve the problem of displaying faults in this model, an approach as suggested by Caumon et al. (2009) was followed. First, a grid surface of the fault itself was created. The fault trace at the surface was taken from the mapped surface geology, and a grid was projected downward from the line at a 30-degree angle, which is a common angle for low-angle thrust faults (Boyer and Elliott, 1982), such as the faults mapped in this study area. Then, two separate models were created and two sets of stratigraphic horizons were developed, one on the hanging wall of the fault, and one on the footwall side.

The fault plane can be thought of as the edge of the model, for the two models on either side. Wells or "ghost boreholes" on the opposite side of the fault than the side being modelled should not be included in the interpolation process. This is so they do not influence the elevation of the unit being interpolated. The elevation will be either higher or lower on the opposite side, due to an abrupt displacement, not an increase/decrease in the dip angle of the formation, which is what would occur if the surface contacts on the opposite side were still used. This method would work for a vertical fault, and does on the hanging wall side of the fault; however this does not work on the footwall side. This is because on this side, below the surface, the units extend beyond the fault trace at the surface. In addition, with triangulation, the last control point is the edge of the model, and if it is a vertical borehole, the surface will end vertically (Figure 5.5a). To rectify this problem, three additional boreholes, with estimated depths, angled with the fault plane, were created (Figure 5.5b).

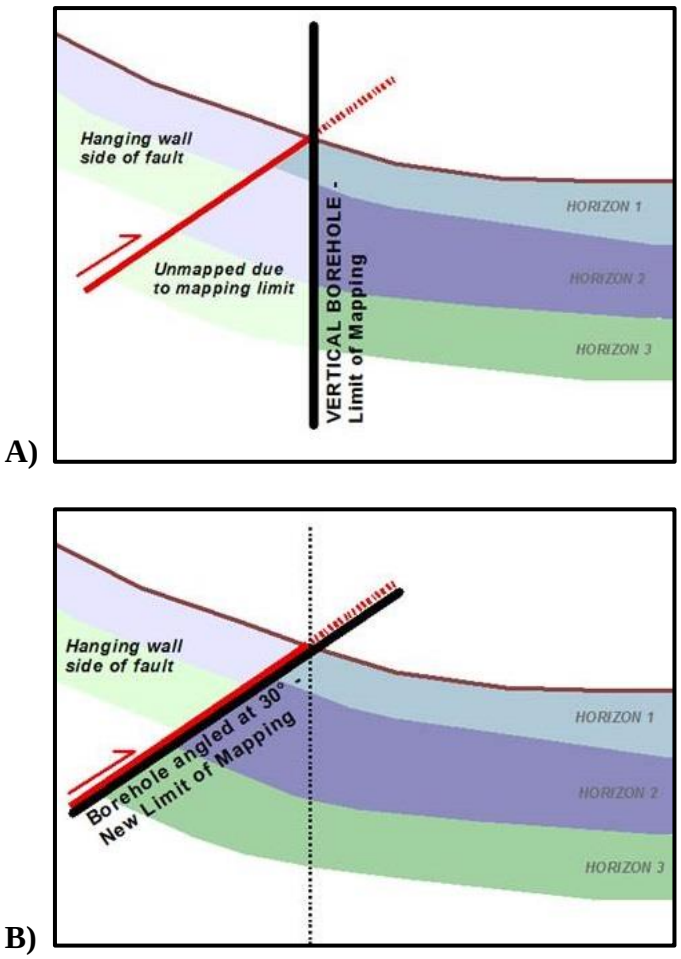

Figure 5.5. Example of thrust fault and a) unmapped area due to vertical boreholes and b) angling the borehole with the fault surface to fix unmapped areas

These two models, on either side of the fault, were then merged together into a single model. In Rockworks17, this was performed by using the fault as a dividing grid surface, and merging the two solid models so that the upper portion of the model (above the fault) becomes the model on the hanging wall side, and the lower model, the footwall side.

5.3.3 Results Assessment

If a synthetic, continuous grid of known accuracy existed, a quantitative assessment could be performed to determine how the interpolated model deviates from this known grid. Not enough observational data is available in this region for this level of detail to be known, however, and creating a model that would be considered accurate enough for the purposes of a quantitative comparison to further models is beyond the scope of this study. The subsurface in this region has only been interpreted by geologists and

consequently any model of it remains an estimation of reality. If a surface whose values have been derived through interpolation itself were used, there would be an inherent propagation of error. Therefore, when attempting to determine spatial interpolation accuracy, only synthetic grids where values are known for every location, should be used (Zimmerman et al. 1999). For this reason, a quantitative accuracy assessment will not be performed.

This results assessment stage for this study can be divided into two phases:

(1) The assessment of the interim model/individual surfaces, and

(2) The assessment of the final model.

The 3D modelling process is an iterative one, where assessing the results and then making progressive refinements to the model are important requirements in the modeling process (Turner, 2006; Zanchi et al., 2007). When the output is unsatisfactory, amendments are made to the inputs and the model re-created.

The results of the interpolation of the individual stratigraphic surfaces were assessed qualitatively. With the assistance of expert geologists, the surface was evaluated for conformity with the current scientific understanding of the subsurface, based on common geologic principles, regional knowledge and published literature. This was particularly important for layers that were not continuous across the study area. For example, layers that outcrop at the surface, or those that pinch out below the surface were given careful examination. If the surface was not consistent with what was expected, it was necessary to add additional controls to the model, and re-interpolate the stratigraphic layer. This required us to return to the "3D Modelling" stage, and re-model the surface using the methods described. For reasons of brevity, not every iteration of this process will be discussed in this paper, only the ones with a substantial impact on the ultimate result.

Once the final model was created, after stacking each individual layer upon the others, the reliability and uncertainty of the final model was assessed. The model reliability definition proposed by McCormack (2010) was used. It states that the model must closely resemble the known stratigraphy and subsurface, be consistent when the model is re-created, conforming to the individual inputs, and is similar in its depiction of the

formations present when compared against outside sources. The reliability of the final 3D model was assessed using those criteria.

The uncertainty of the final model was depicted solely as a function of data density in 2D space. For this study, as the main inputs are all in-situ measurements (boreholes), we can assume that the further we are from one of these known points, the higher the uncertainty is in the resulting interpolation. A gridded surface was created with values increasing with distance from the borehole. Data density is often one of the inputs to an uncertainty assessment that examines multiple criteria, used alone it is generally not comprehensive enough to assess uncertainty in a 3D environment. It is noted that the data density requirements rely heavily on the complexity of the terrain. However, it still allows users to see easily where the uncertainties in the model might exist, due to lack of measured data. .

6.0 RESULTS

The results section has been broken down in three main sections, similar to the three stages of the modelling process described in the methods. The first section below describes the results of the data set-up process where applicable, the second one outlines the results of the interim surfaces from the modelling process and Horizons Method, and the third section describes the findings from the results assessment of the final model.

It should be noted, that the focus of this paper is not on the geological interpretation of the Mackenzie Plain, rather it is on the methods and techniques used for the modelling. The geologic deductions made in this paper, although following general geological principles, have not been reviewed by any professional geologists.

6.1 Data Preparation / Set Up

6.1.1 Data Compilation and Derived Thickness Estimates

After the data was compiled and reconciled, there were 22 complete boreholes across the whole study area (19 from original NEB well database and three completely inferred on the fault plane), with 170 “ghost” wells created along surface contacts (Figure 6.1; Appendix A).

Only four of the nineteen wells recorded complete depths down to the top of the Saline River formation (the oldest unit modelled), therefore depths had to be estimated for one or more stratigraphic units in the remaining fifteen.

As previously mentioned, using seismic data in addition to the well picks, subsurface elevations could be estimated down to, at minimum, to the top of the Hume formation. The understanding that the thickness of the Hume formation is fairly consistent across the study area is supported by data from the wells. Although there are two wells where the thickness is considerably higher or lower than average, 176 meters and 81 meters respectively, most are within 20 meters of one another. The average of all the values across the study area is 130 ± 19.9 meters. In wells which do not have a bottom depth recorded, this average value of 130 meters was used to determine its bottom depth, which corresponds to the top of the Bear Rock formation.

The Bear Rock formation thickness varied slightly more than the Hume formation across the study area, by approximately 50 meters. The average depth for this formation is 346 meters ± 50 meters. However, due to the higher variation, an average of the two closest wells was taken, rather than the average from the entire study area. These values range from 250.1 meters to 377.4 meters (Appendix A).

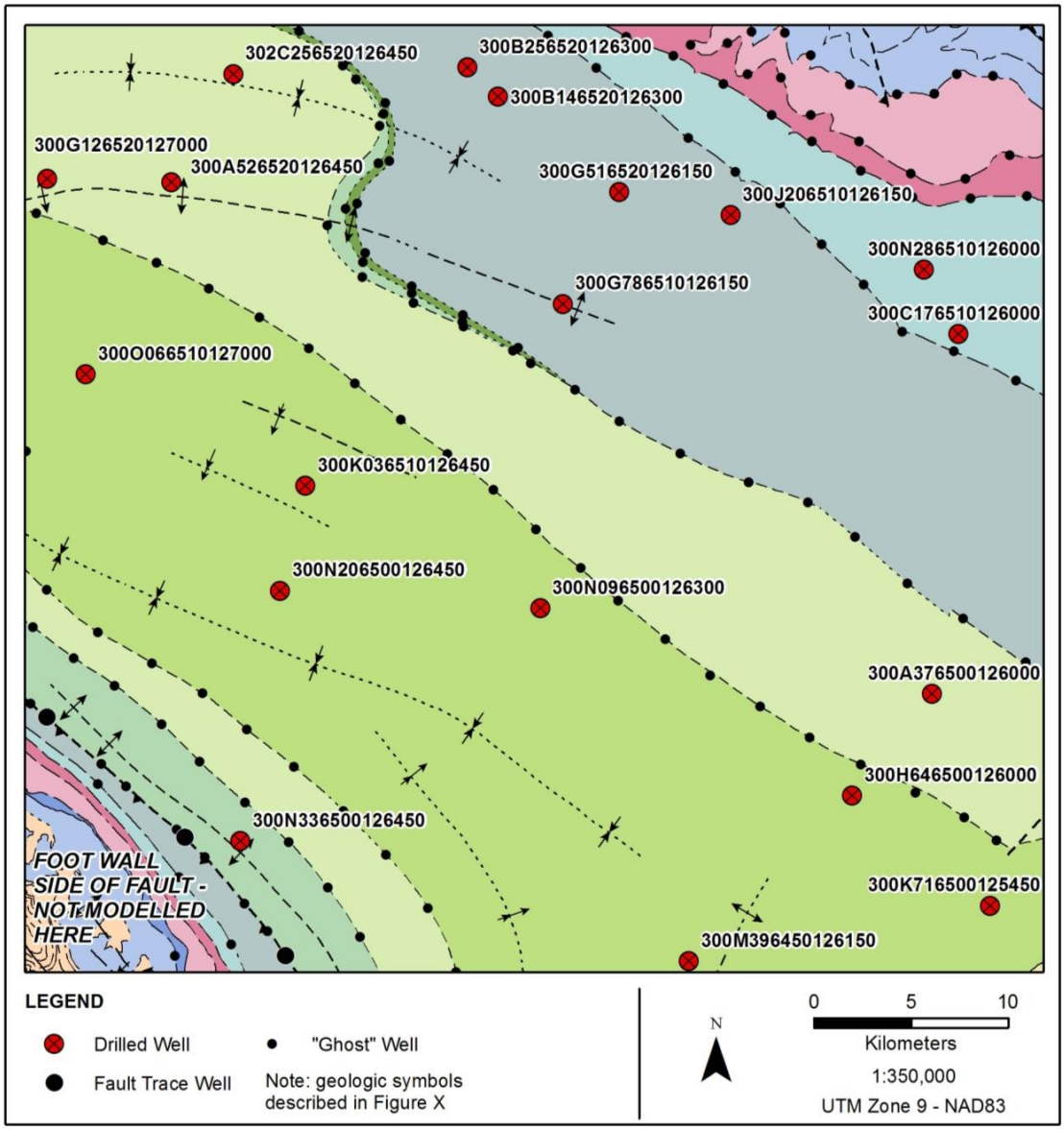

Figure 6.1. Location of wells and ghost wells with geology in study area

Two measured sections, surveyed just outside the southwest boundary of the study area in the Mackenzie Mountains, record a Mount Kindle formation thickness of 135 meters and 140 meters (Pope and Leslie, 2013). Therefore, a thickness of 140 meters at the

edge of the study area in these ranges is assumed, and that it pinches out at the midpoint between the well with its last known location, and the wells in which it is not present.

Finally, the Franklin Mountain formation thickness values were estimated using mostly qualitative geologic knowledge. Maximum thickness in the Mackenzie Mountains, just west of the study area, was found to be 525 meters in a measured section, and around 280 meters in the Norman Range, just north of the study area (Turner, 2011). In addition, it was found to be 224 meters in a well just east of the study area (UWI 300A496500125450). Therefore, approximate values were used in the wells, ranging from 500 meters and thinning out to 200 meters in the northeast.

The final stratigraphic depths calculated for all units in every well can be found in Appendix A.

6.2 Modelling Process

The modelling results are described and assessed in three different phases: individual stratigraphic surfaces/unit thicknesses, the merging of the surfaces into a model without a fault, and the final model with a fault incorporated for consistency with the published bedrock map (Fallas et al., 2013).

For simplicity, the results presented for the first two phases are only on the northeast, or footwall, side of the fault; which comprises the majority of the model. The results and theory of the interpolation on either side of the model were similar, so the results presented on one side are applicable to the other.

6.2.1 Individual Surfaces

To best illustrate the creation of individual stratigraphic surfaces, the results are presented for a well-constrained stratigraphic unit: the Hume formation. This unit is present across the study area except beyond where it outcrops at the surface in the northeast and southwest corners, and it has a relatively uniform thickness across the area. As the interpolation of each surface behaved in a similar manner, it is possible to single out one unit and use it as a representative surface.

6.2.1.1 Inverse Distance Weighting (IDW)

In general, surfaces created by IDW are undulating with a strong bullseye effect. That is, there are very pronounced highs and lows at control points. This effect is most visible

in a cross sectional view, between two wells with no other control between the two (Figure 6.2). Rather than have a straight line from one well elevation point to the next, we see a slight curve in the line, which gives the impression of folding between wells, which is not consistent with seismic data or geologic knowledge of the region.

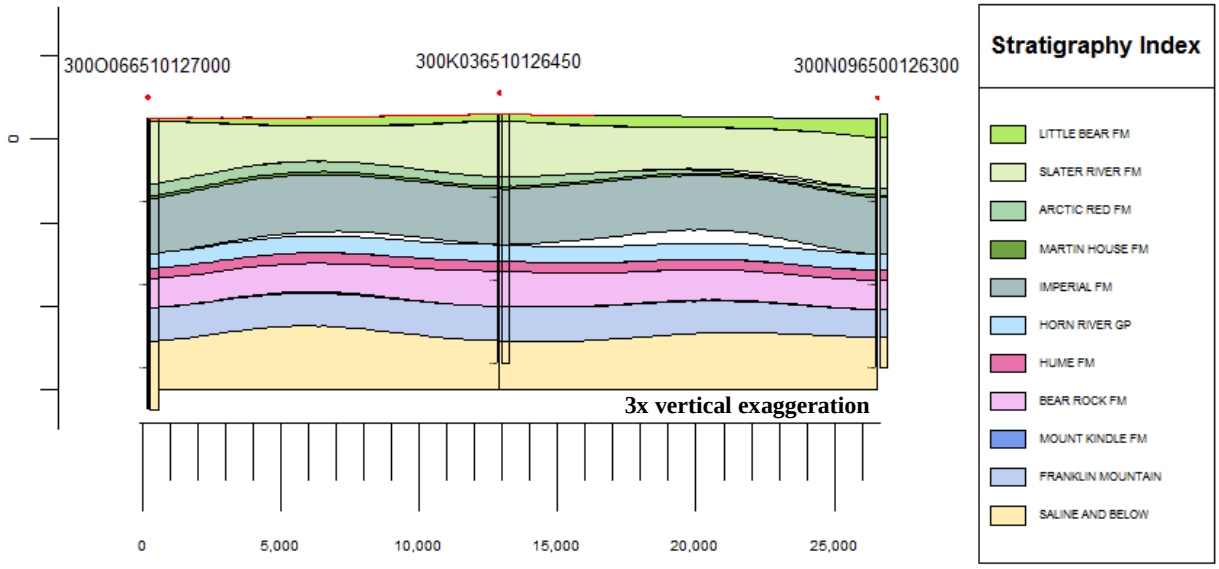

Figure 6.2. Cross sectional view of IDW model between wells 300N206500126450 and 300N096500126300

Decreasing the weighting exponent to one, from a default value of two, a more pronounced bullseye effect is seen (Figure 6.3a). Increasing it to three, the effect is lessened and the surface less undulating (Figure 6.3b). This surface appears more like a surface with a smoothing filter applied (Figure 6.3c). There is little change when the number of neighbour points is changed, unless it is changed to only a single point, in which case the surfaces are essentially nonsensical, as it takes into account only a single neighbouring point.

With an application of a 3x3 cell-smoothing filter, the bullseye effect is reduced slightly (Figure 6.3c). This surface looks more like the surface with a higher weighting exponent, but before the smoothing filter.

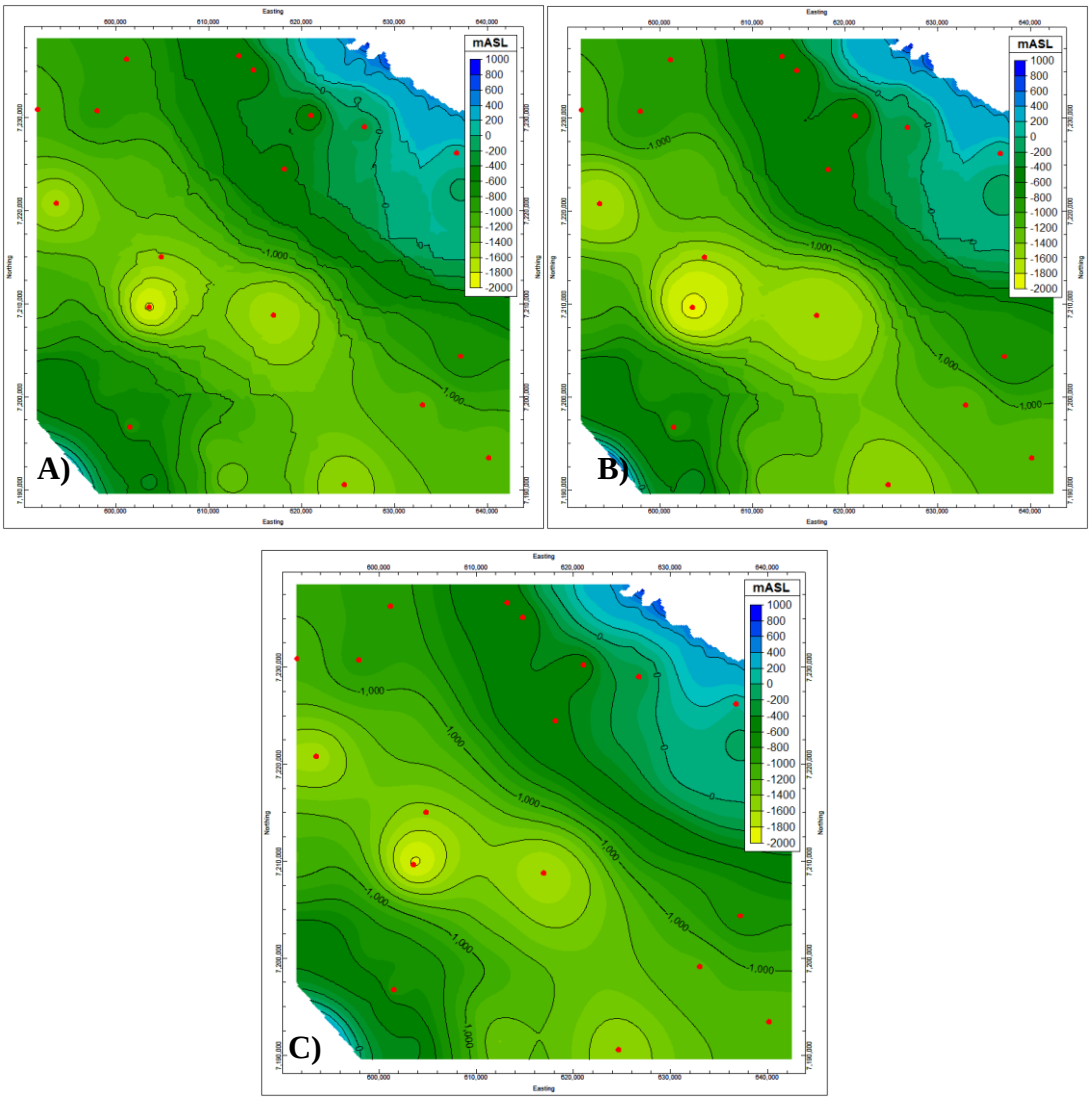

Figure 6.3. IDW interpolation of Hume formation top using exponents of a) one, b) three, c) two and 3x3 smoothing filter.

The optimal number of points, based on a qualitative assessment of the most geologically realistic surface, is determined to be achieved using a weighting exponent of two with the default number of points (8), and a 3x3 cell smoothing filter (Figure 6.3c). However, the stratigraphic surfaces still vary in a very uncharacteristic fashion for a geologic surface in this region. Undulations, such as those seen in the modelled cross-sections, are not present in the seismic survey data, except where folded, and therefore are not likely characteristics of the actual surfaces in this region.

6.2.1.2 Kriging

The resulting surfaces produced by a kriging interpolation are immediately smoother than those produced by IDW, with a less prominent bullseye effect.

The Hume formation was modelled very well with kriging, even before a smoothing filter was applied. Using the default number of six neighbours, with no smoothing filter, the result has showcased some angular contours, as well some sharp edges, but there was little appearance of a bullseye effect (Figure 6.4a). Increasing the number of neighbours to fifteen yields even smoother results, with only one small area of sharp elevation change in the northeast (Figure 6.4b). This was a fairly geologically reasonable result and did not need a smoothing filter applied. In fact, it was smoother with less jagged edges than even the 6 neighbour interpolation, after a 3x3 cell smoothing filter was applied (Fig. 6.4c).

The results with the modelling of the Hume formation were positive, however, the kriging interpolation did not do as well with all other surfaces. Examining the other formation surfaces, we can see that some, particularly those that vary a lot or pinch out (Arctic Red, Martin House and Mount Kindle formations) had very large undulations and overlaps between surrounding layers (Figure 6.6). The other surfaces, however, were modelled better with kriging (smoother, less undulating) than with IDW.

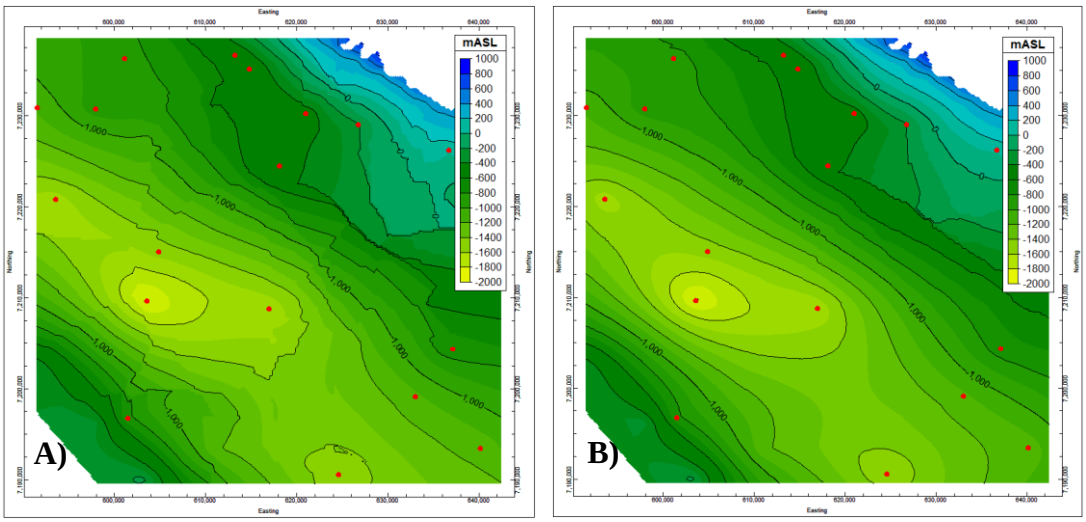

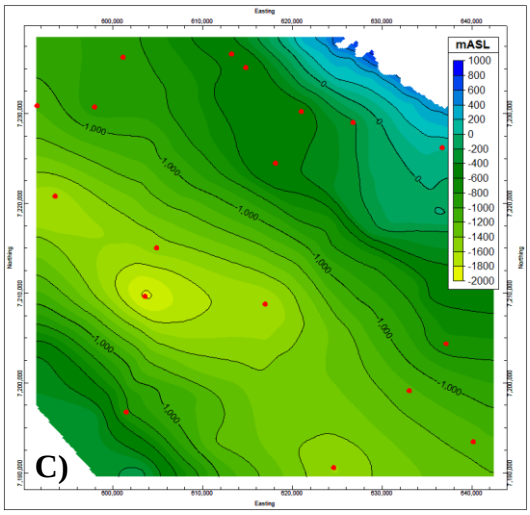

Figure 6.4 a) Kriging of Hume formation top and well locations (in red) using a) 6 neighbours, no smoothing, b) 15 neighbours, no smoothing, and c) 6 neighbours and 3x3 cell smoothing

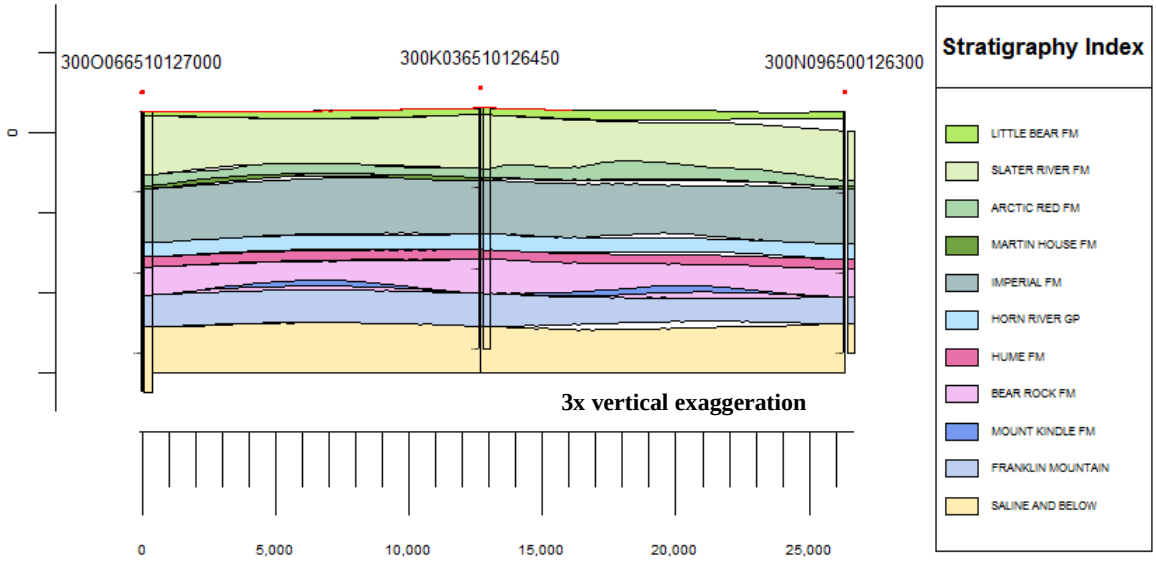

Figure 6.5. Cross section of model using Kriging interpolation, using 6 neighbours after smoothing

The details of the automatically created variograms, within Rockworks17, can be found in Appendix B.

6.2.1.3 Triangulation

The surfaces produced by triangulation are more angular, and less rounded, as compared to both IDW and kriging. This is more like what a surface would look like if one were to draw a straight line between two control points. Before the smoothing filter is applied, the results are quite blocky in appearance and some areas show sharp changes in elevation below the surface – almost fault-like (Figure 6.6a). After a smoothing filter of 3x3 cells is applied, the surfaces are smoother, with less of a "bullseye" effect as seen with the IDW and kriging (Figure 6.6b). These surfaces produced by triangulation, with the smoothing filter, are most like those that a geologist would draw by hand, without superfluous curves in the surfaces.

Note that this algorithm does not extrapolate beyond any control points, so corners or edges are often cut off, depending on where the wells are located. This is why the study area looks smaller and no longer rectangular.

The cross-sectional view shows us the smoothest surfaces yet, and flattest (which is expected in this section), and there are much fewer gaps between surfaces as compared to both IDW and kriging (Figure 6.7).

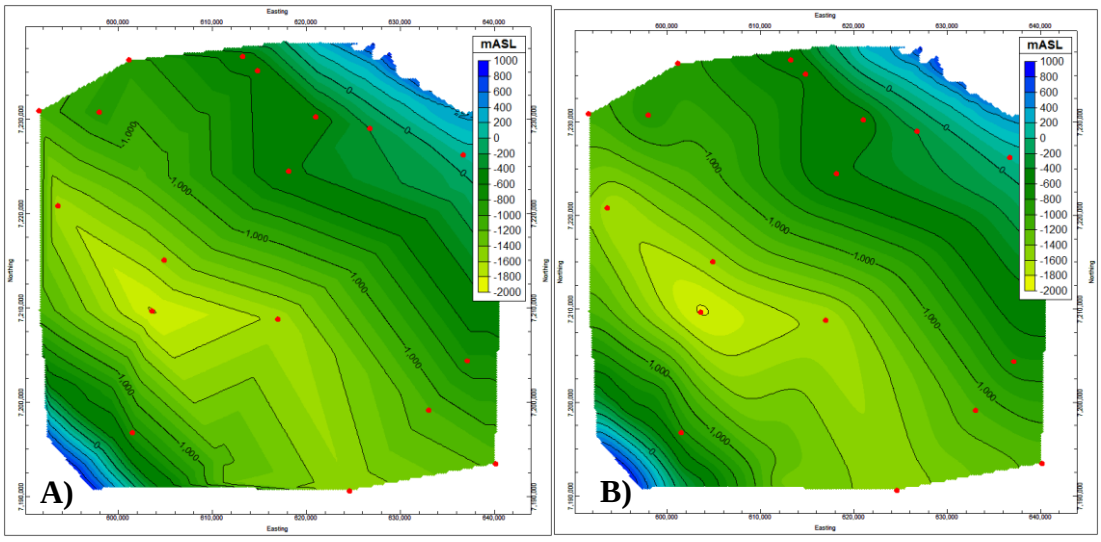

Figure 6.6. Triangulation of Hume formation top and well locations (in red) a)before smoothing filter, b) after smoothing filter

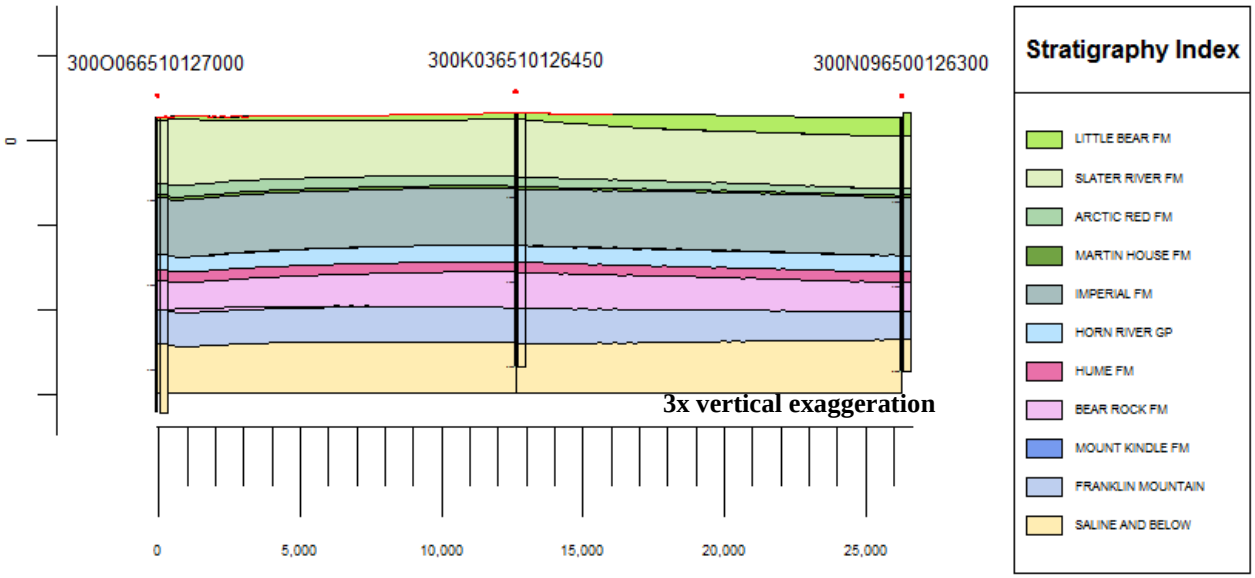

Figure 6.7. Cross section of model using triangulation and smoothing filter

The most appropriate interpolation algorithm is determined to be triangulation. This was the most appropriate algorithm because it conforms to the mapped geology better and generates a well-defined syncline axis, rather than patchy low or high spots seen with the others.

6.2.1.4 Hard to model surfaces

Martin House, Arctic Red, and Mount Kindle formations all pinch out below other units in certain areas and are present in other locations, making an accurate representation more difficult where there are no boreholes to constrain the pinch out locations.

Martin House formation is the thinnest modelled unit in the region, reaching a maximum of 40 meters, according to the well data. Surface mapping shows that the unit comes up to the surface in the north, and pinches out below the surface in the south (Figure 6.1). Modelling the top and bottom of the unit, and calculating the thickness in between, it can be seen how well the thickness of that unit was interpolated.

The IDW interpolation algorithm, with a smoothing filter, results in surfaces that mirror what the expected thickness should look like. That is, generally continuous at 25-35 meters, and pinching out to a thickness of 0 towards the northeast (Figure 6.8a). There are a few areas where the top and bottom surfaces overlap and the thickness goes to 0, and then it thickens again, which is a function of modelling errors, and is not

geologically likely in this region. Once again, a bullseye effect is seen, and there is an area in the north where the unit outcrops and the thickness goes down to 0, however should be greater than 0. The exact position of the northeast edge where it pinches out shows a fair amount of irregularity, and has very sharp changes in thickness, seen by the jagged contours. Although a feature possible in reality, in this case it is likely an artefact of the modelling method and not justified by control points.

The kriging interpolation algorithm resulted in surfaces that were not geologically realistic for this region, nor did they resemble any other surfaces produced by the other two interpolations (Figure 6.8b). In the three formations that pinched out, there were extreme undulations and the thickness went to zero in numerous locations, in between well control points. There was also a sharp increase in thickness in several areas, much beyond what was geologically reasonable. The kriging interpolation algorithm resulted in a similar surface to IDW, although it was slightly smoother, and even appears to be slightly more undulating (Figure 6.8b). There are also some areas of geologically uncharacteristic thickening, such as in the south and northwest. On the other hand, the kriged surface is modelled better in the north where the unit outcrops – only a minor "bleeding" of the unit occurs, as compared to IDW. The sharper decrease in thickness is more realistic as the thickness should remain fairly consistent until it outcrops and immediately goes to zero.

As with the other individual surfaces, triangulation, with a smoothing filter, results in the most geologically acceptable surface representation (Figure 6.8c). Less undulating and more linear between control points, it conforms better to geologic rules and the regional knowledge of the area. The irregularity in the unit thickness near where the unit outcrops is also not as evident.

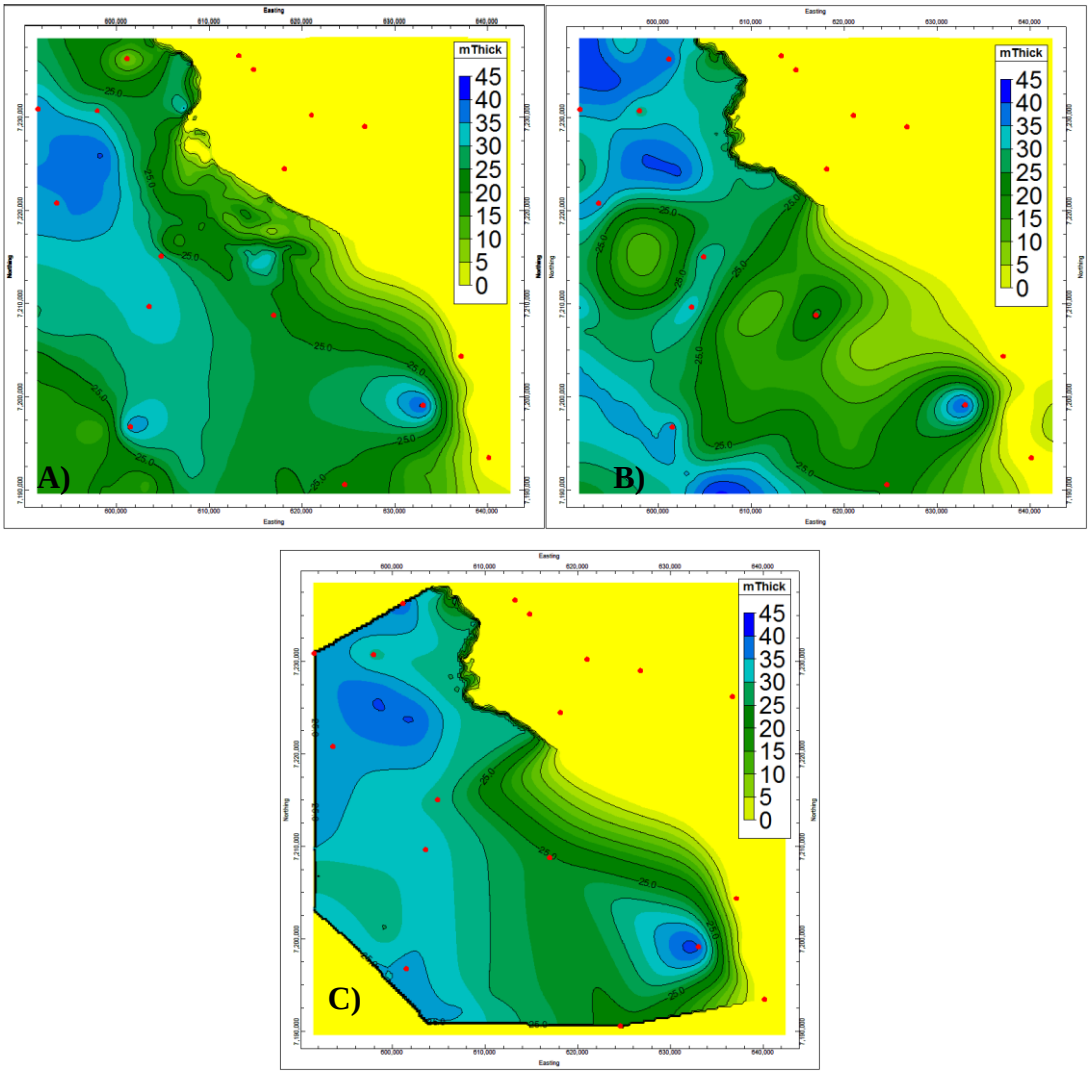

Figure 6.8 Martin House formation thickness grids interpolated by a) IDW with smoothing filter, b) kriging with smoothing filter and c) triangulation with smoothing filter

The Arctic Red and Mount Kindle formation surfaces behave in a similar manner to the Martin House formation. Triangulation, once again yields the most acceptable results, however still not perfect, therefore minor manual edits were necessary to avoid obvious geological inconsistencies. Particularly where it outcropped at the surface, or if an uncharacteristic thickening or thinning after gaps and/or overlaps were removed, was present.

6.2.2 Model Without Faults

6.2.2.1 Intersecting layers

As can be seen in the cross-sections in the previous sections, there are often some overlapping units, or small gaps between the layers, between well control points (Figure 6.9). When all the horizon elevations are intersected with one another and adjusted to the unit below, there are no longer any gaps or overlaps between units. The result of the adjusted elevations across a small cross-section can be seen in Figure 6.10.

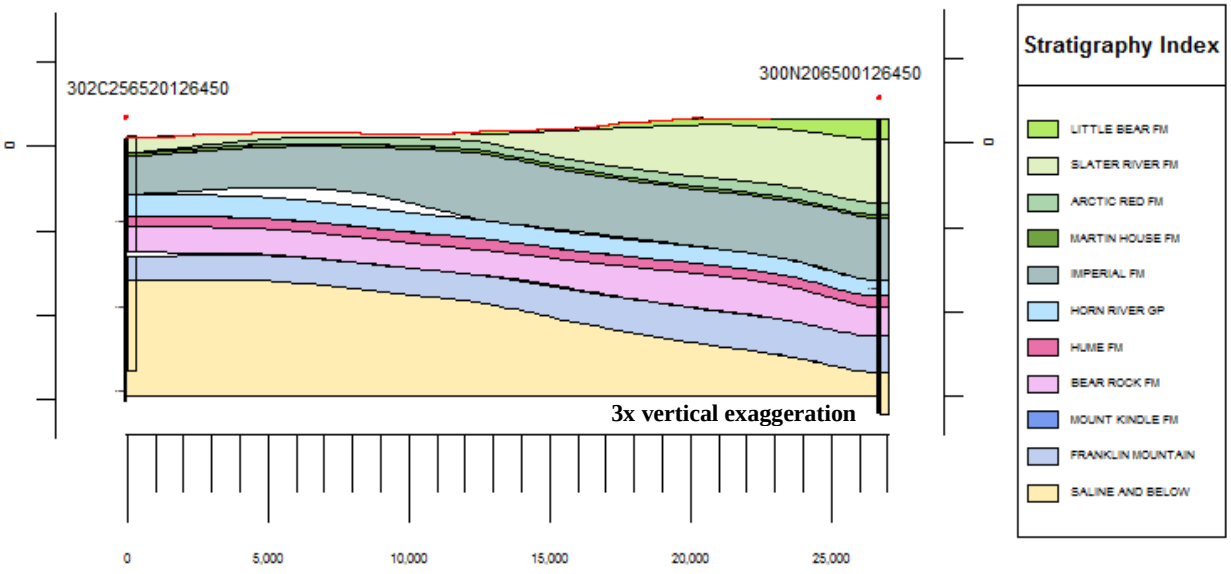

Figure 6.9. Gap presents between Horn River Group and the above Imperial formation

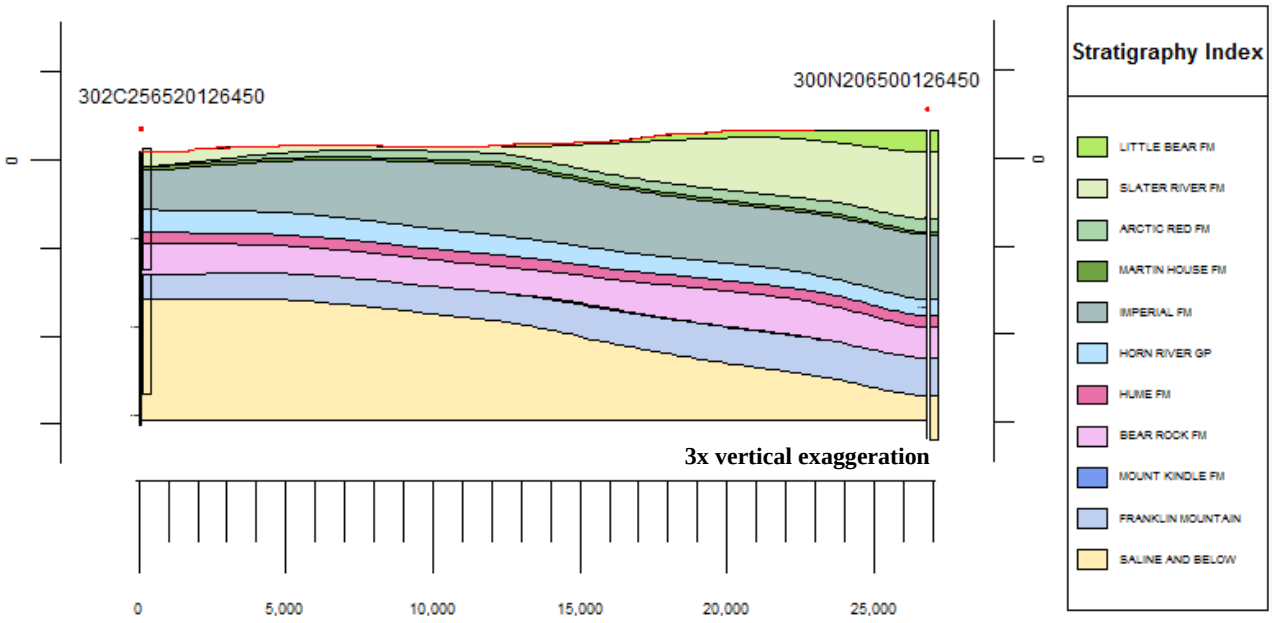

Figure 6.10. Adjusted stratigraphic surface elevations to remove gaps and overlaps

Changing the bottom elevations of units to eliminate overlaps, however, results in changes to their thickness values and is especially evident in the hard to model units (e.g. those which pinch out or are thin). Units whose thicknesses were previously modelled acceptably, can become geologically unrealistic. For example Arctic Red formation, which had a fairly realistic pinch-out below the surface before adjustment, afterwards has two unlikely holes, due to overlaps with the surface below that take precedence (Figure 6.11). Or, if a gap exists between units, the thickness of one unit is increased, to reach the top of the unit below. The thickening of the Arctic Red formation near the fault in the southwest is not an alarming feature – the thickness of the unit is increasing towards the west, and its thickness is greatest as it outcrops. It then decreases as the bottom surface of the unit trends towards the surface (Figure 6.12).

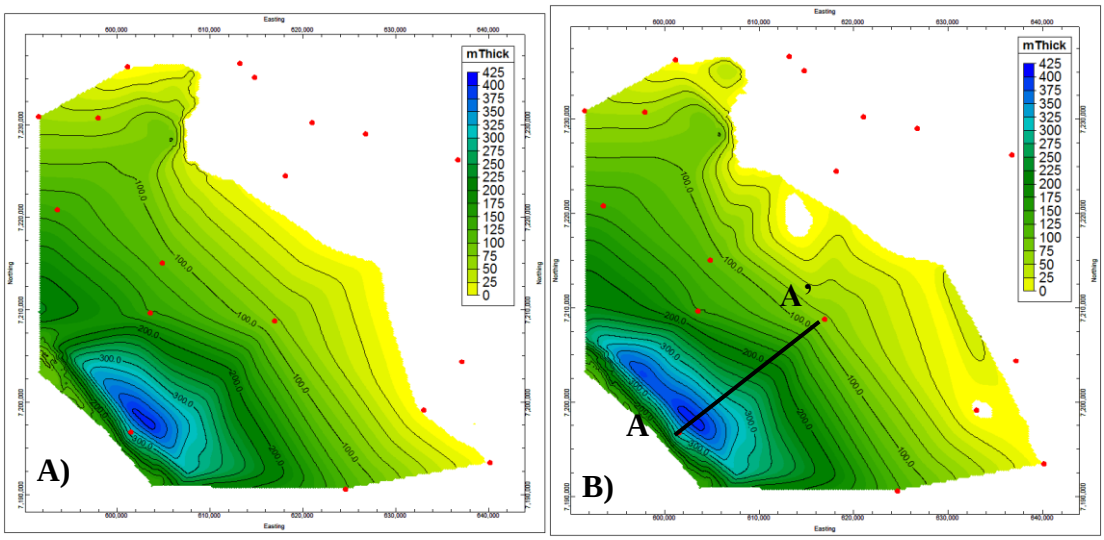

Figure 6.11. Arctic Red formation a) before overlaps/gaps fixed; b) after overlaps/gaps fixed, with cross-section line for Figure 6.11

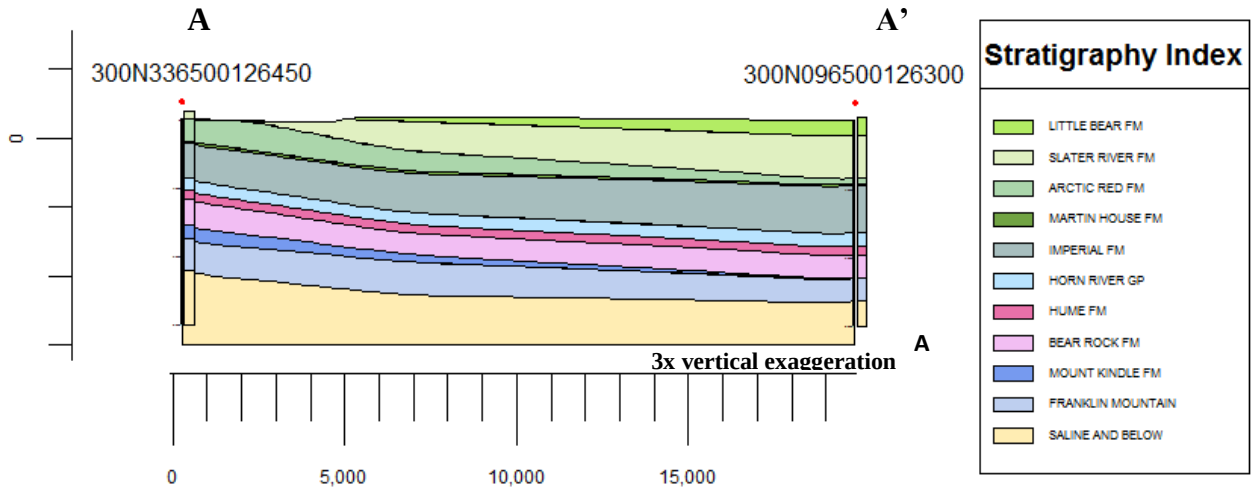

Figure 6.12. Cross-section of section in Figure 6.11b

6.2.2.2 Manual Edits

Manual edits on thin units, or those that pinched out below the surface in a geologically unrealistic manner after the horizon intersections, was necessary. The two units affected by a subsurface pinch out, and which required manual edits, were the Arctic Red and Mount Kindle formations. The pinch out modelled for Martin House was considered to be plausible.

It was also necessary to perform manual edits of each of the surfaces that outcropped at the surface due to the bleeding or undershooting of units (Figure 6.13a). Most units experienced some sort of bleeding effect. These edits were minor (not changing elevations more than a few meters) and were mainly done for cartographic purposes to ensure the modelled contacts lined up exactly with the mapped contacts. After the manual edits were performed, the units seen at the surface matched with the geologic map polygons as published (Figure 6.13b).

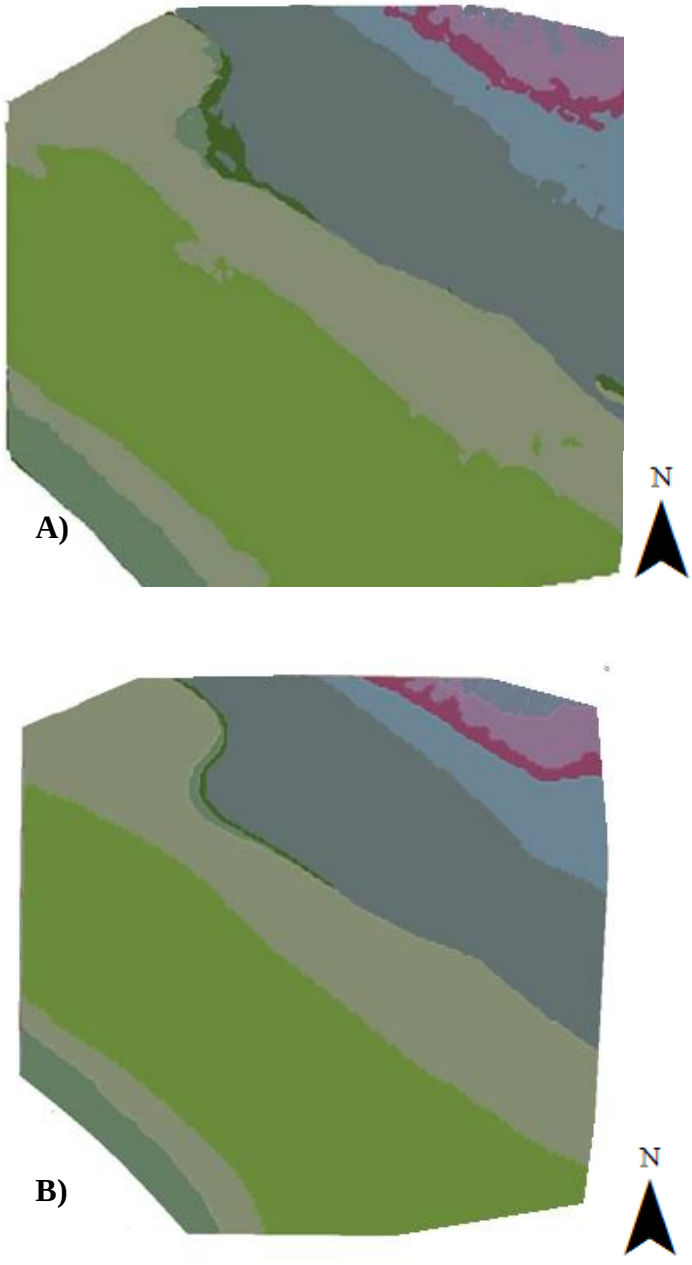

Figure 6.13. Model results a) before and b) after surface edits.

6.2.3 Model Merged With Faults

The fault going through the southwest corner of the study area is interpreted as a low-angle thrust fault, dipping southwest, as in Fallas et al. (2013) (Figure 6.14).

The result of the two models on each side of the fault, after being clipped to the fault surface, can be seen in Figure 6.15. This is the final model of the area.

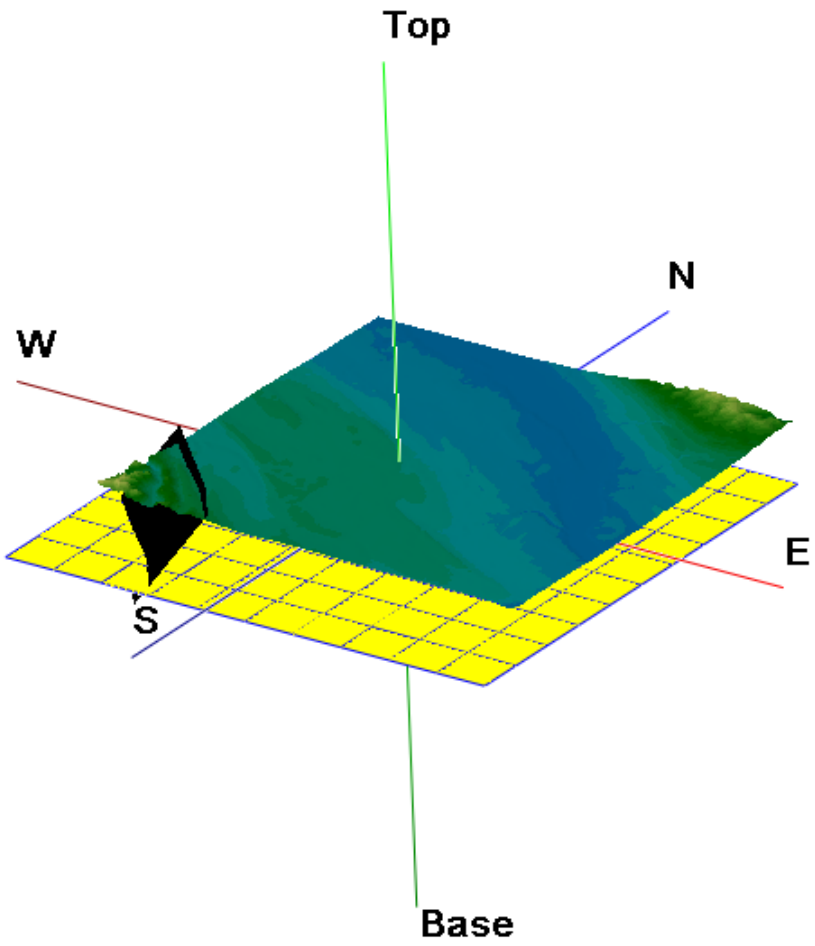

Figure 6.14. Modelled fault surface (black plane) and DEM (blue-green gradational)

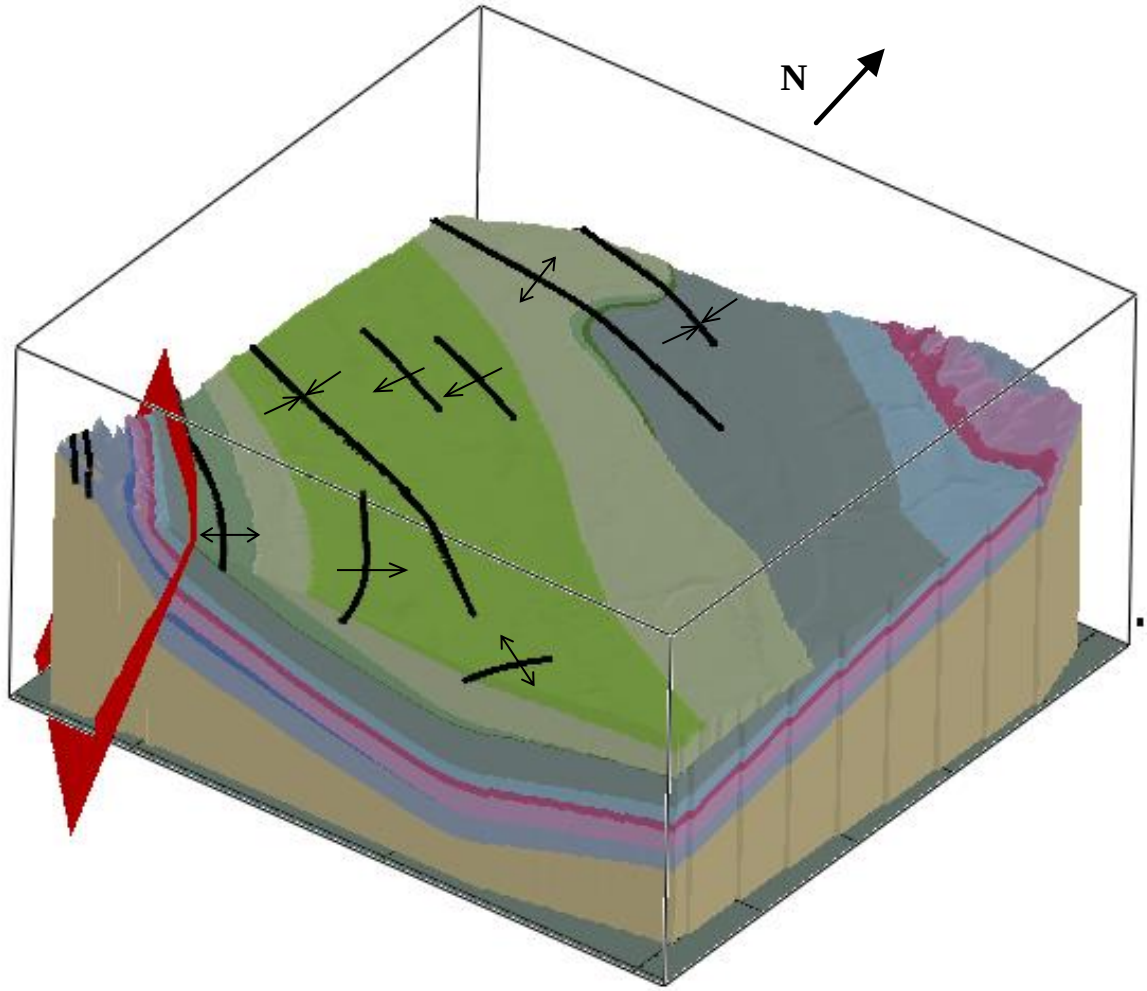

Figure 6.15. Final merged solid model with 5x vertical exaggeration; fault plane appears as red surface.

6.2.4 Creating the Solid Model

Once the model was complete, the top and bottom surfaces were extruded and a solid voxel model was created. The resulting voxel model was much blockier in appearance when zoomed in, which is an artefact of the cell size used (Figure 6.16).

Figure 6.16. Voxel model of study area in Mackenzie Plain

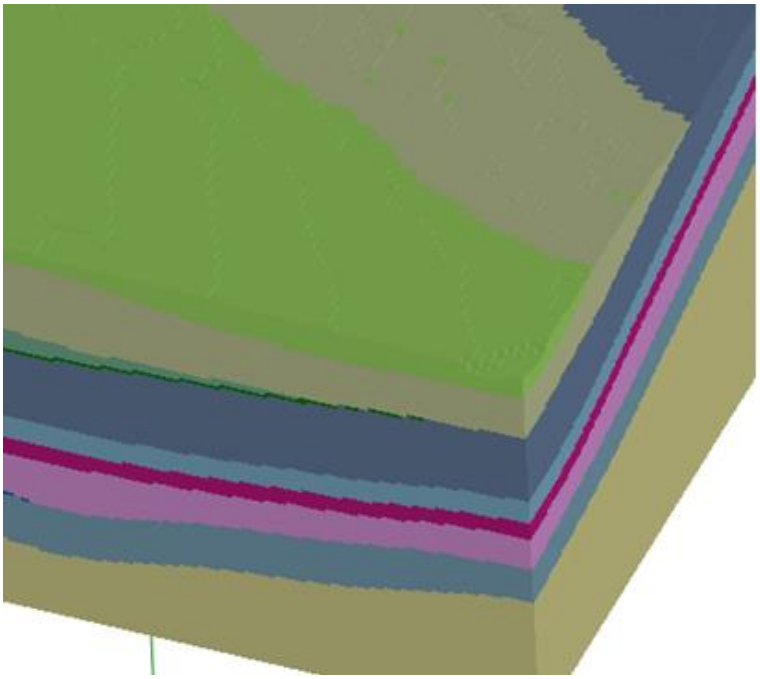

Figure 6.16. Close up of southeast corner of voxel model, with 5x vertical exaggeration

6.3 Results Assessment / Model Uncertainty

The model was assessed for its reliability using the definition as stated in Section 5.3.3: Results Assessment

Using mapped structural features, it is possible to determine where and approximately what a fold or a fault should look like in the subsurface. In this model, we can see that a syncline is present, however the bottom of synclinal trough does not exactly line up with the fold mapped at the surface (Figure 6.17). We also see in the north side of the model the start of a change in bedding inflection, however, it is minor. The less prominent folds (e.g. monoclines) are also not captured in the subsurface in this model.

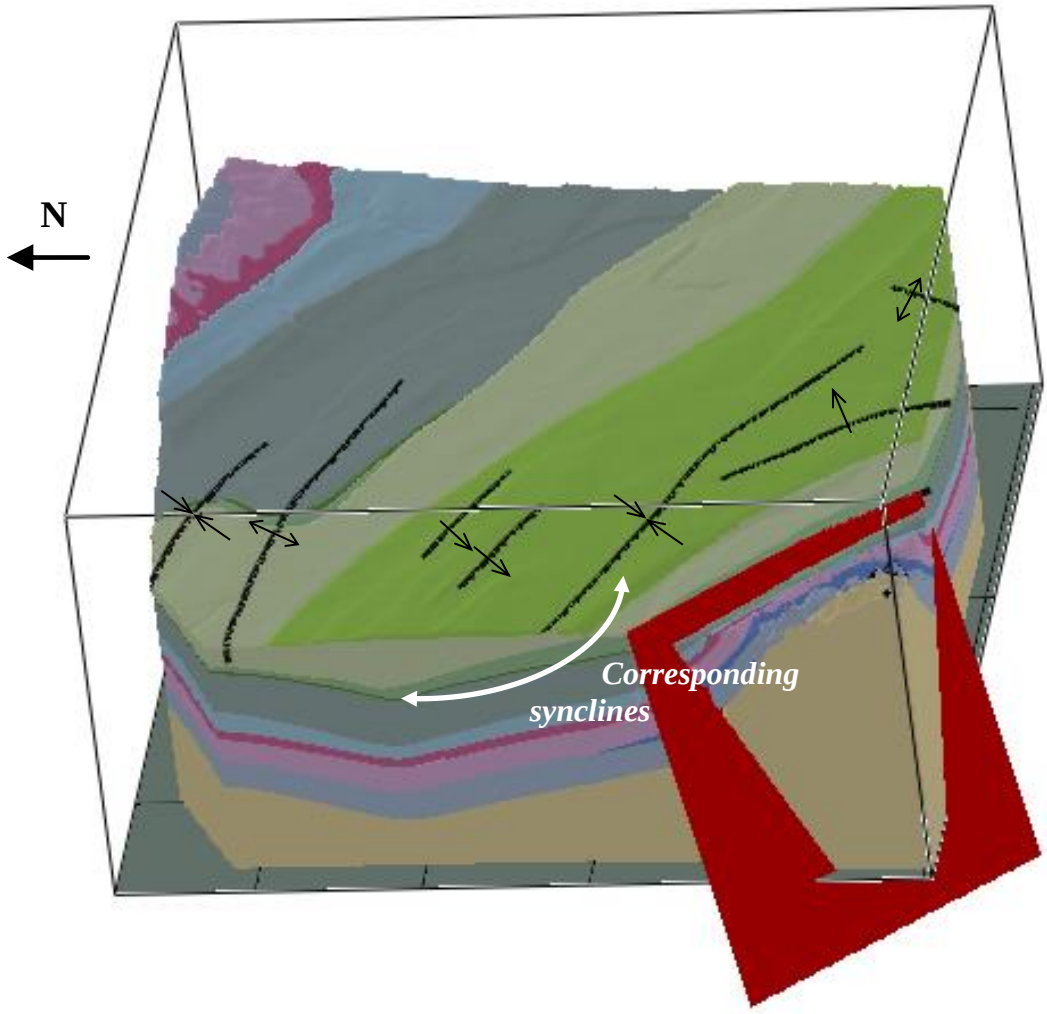

Figure 6.17. Final model with mapped structural features, with 5x vertical exaggeration

If the model were to be re-created by a different user, with the same original input data, it might differ from the model presented here due to the steps involving manual edits and depth estimates required. Therefore, it is not possible to say that a re-created model would conform 100% to the original. However, if the same geologic knowledge and principles were used when performing the edits, it could be very similar, if not almost identical.

The model does conform to the individual inputs. The interpolation algorithm used is one that honours all inputs, and the model was manually edited to ensure it conformed to the published geologic contacts at the surface.

Proxy sources for this modelling exercise included data derived from interpreted seismic surveys. A comparison between a representative seismic section (w13-97-14) and a cross-section through the model at the same location, illustrates where the modelling does and does not correspond to the seismic data image (Figure 6.18). As the seismic images are in two-way time rather than depth, only the general shape of the structures in the subsurface can be compared, however the cross-sectional view highlights some important features. It can be seen that the general shape of the Twentyfive Mile Lake syncline is similar in the modelled surfaces along this cross-section, although once again, the deepest part of the trough does not appear in the exact same location – it appears too far north. We can also see evidence of the Loon Creek anticline, although once again, slightly off in its location. Smaller monoclines are also visible in the seismic section, but were not captured well in the modelled surfaces (Figure 6.19).

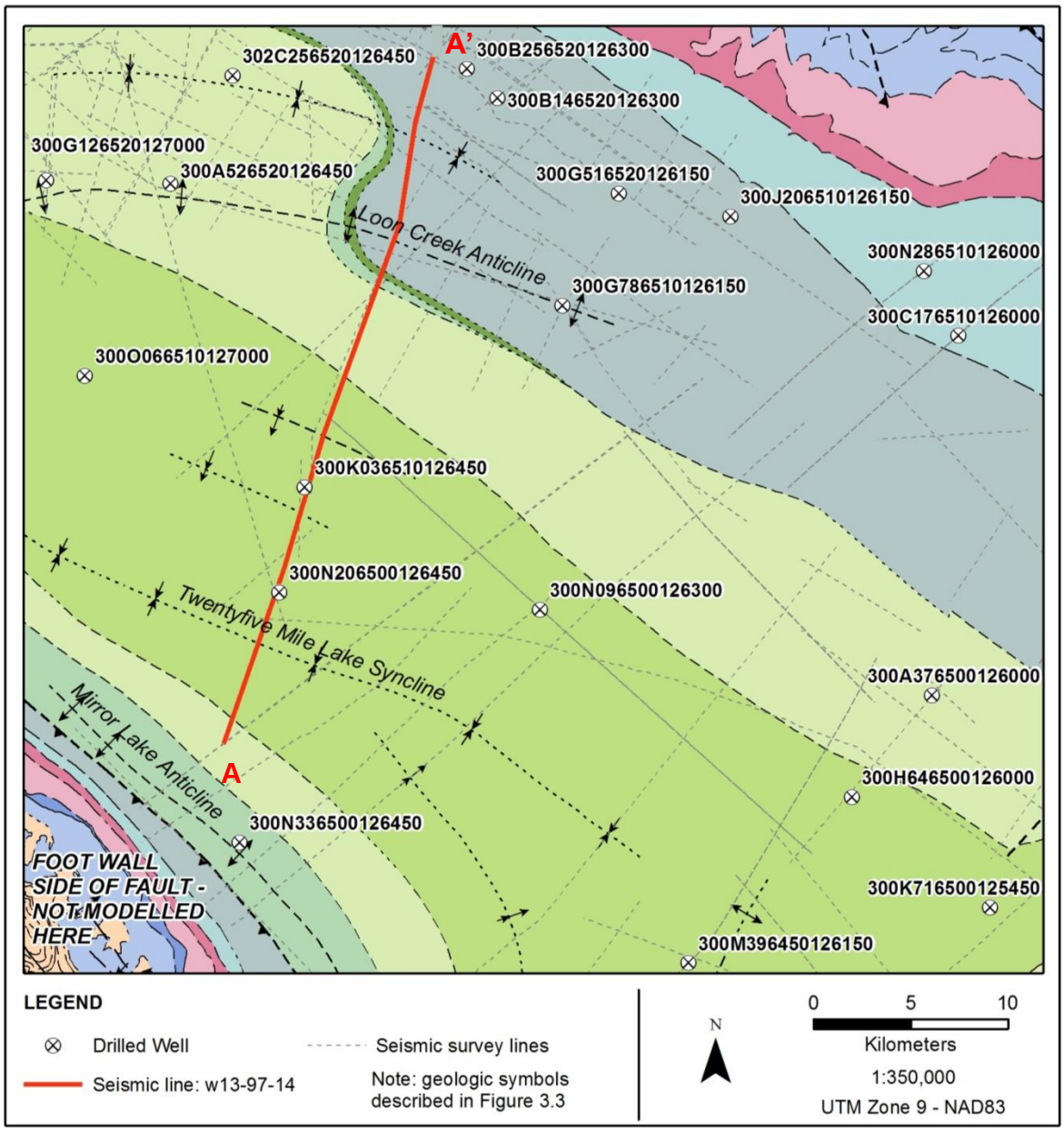

Figure 6.18. Location of seismic survey line

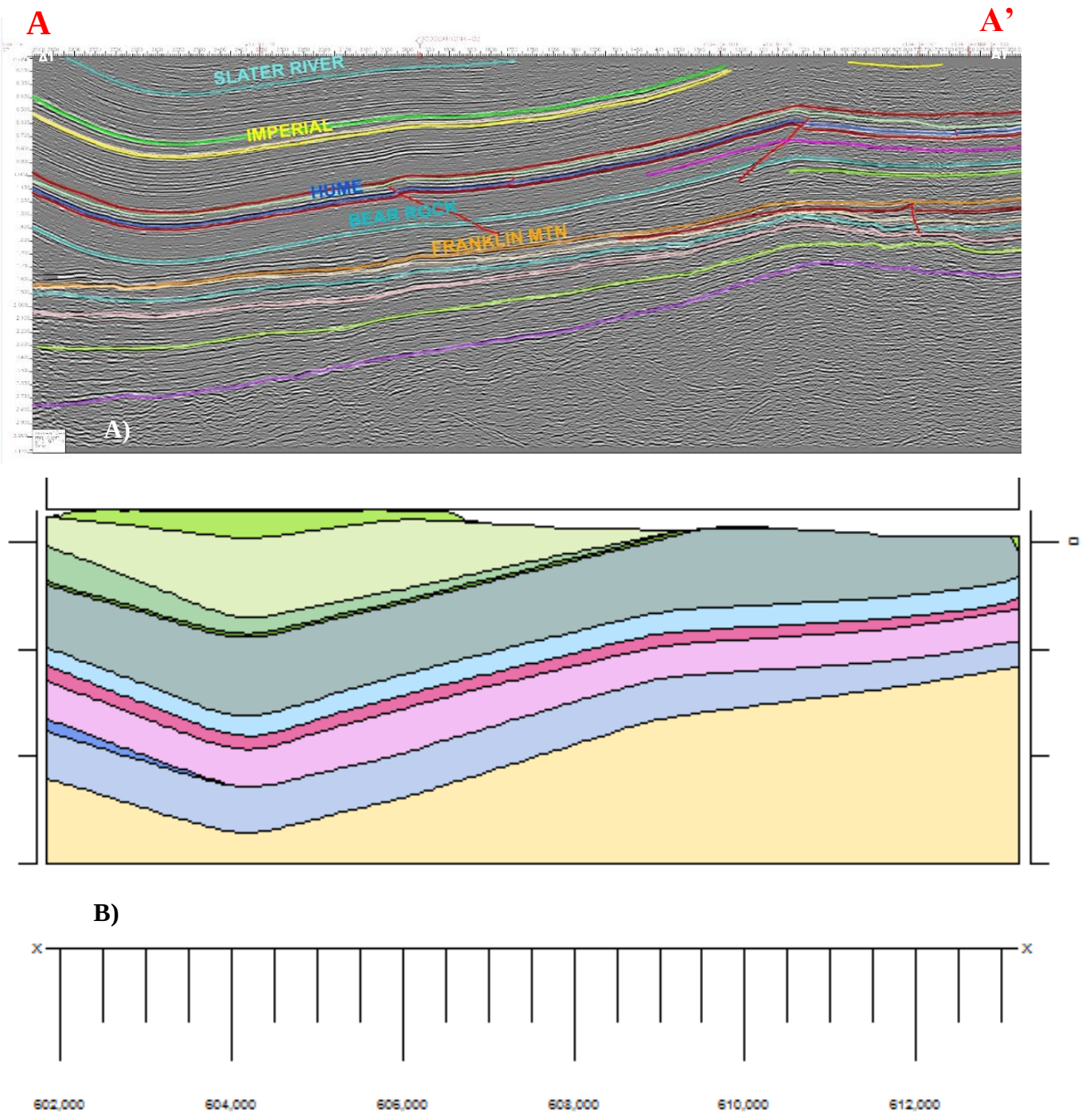

Figure 6.19. Cross section from a) seismic image, lines denoting top of formation surfaces, and b) modelled from Rockworks. These images are coincident with one another from left (A) to right (A')

Due to the fact that only two of the four reliability criteria are satisfied, it is not possible to say the model is completely reliable. Although the extent to which the model conforms with the known stratigraphy and subsurface is subjective, it was concluded that due to the errors in properly modelling the folds, this model does not *closely*

resemble the known geology. It is also not possible to say that a re-created model will be consistent with the original, due to the manual intervention. The model does, however, conform with individual inputs and is similar to proxy sources (e.g. seismic).

In terms of uncertainty due to distance from control points/lack of data density, we can see that the areas of highest uncertainty are in the northeast corner of the study area, and several locations through the centre (Figure 6.19). Although one area in the centre of the model does not have a lot of geological complexity, and therefore may not need many control points, several of the other areas of high uncertainty, also exhibit a higher geological complexity (several units outcropping at the surface and folding occurring). These are areas which would require high data density for accurate modelling. The presence of outcrops can also be considered a control, and would reduce uncertainty as we use these locations as “ghost” wells, however as they only give a single surface either a top or bottom value, they only reduce the uncertainty for that one surface.

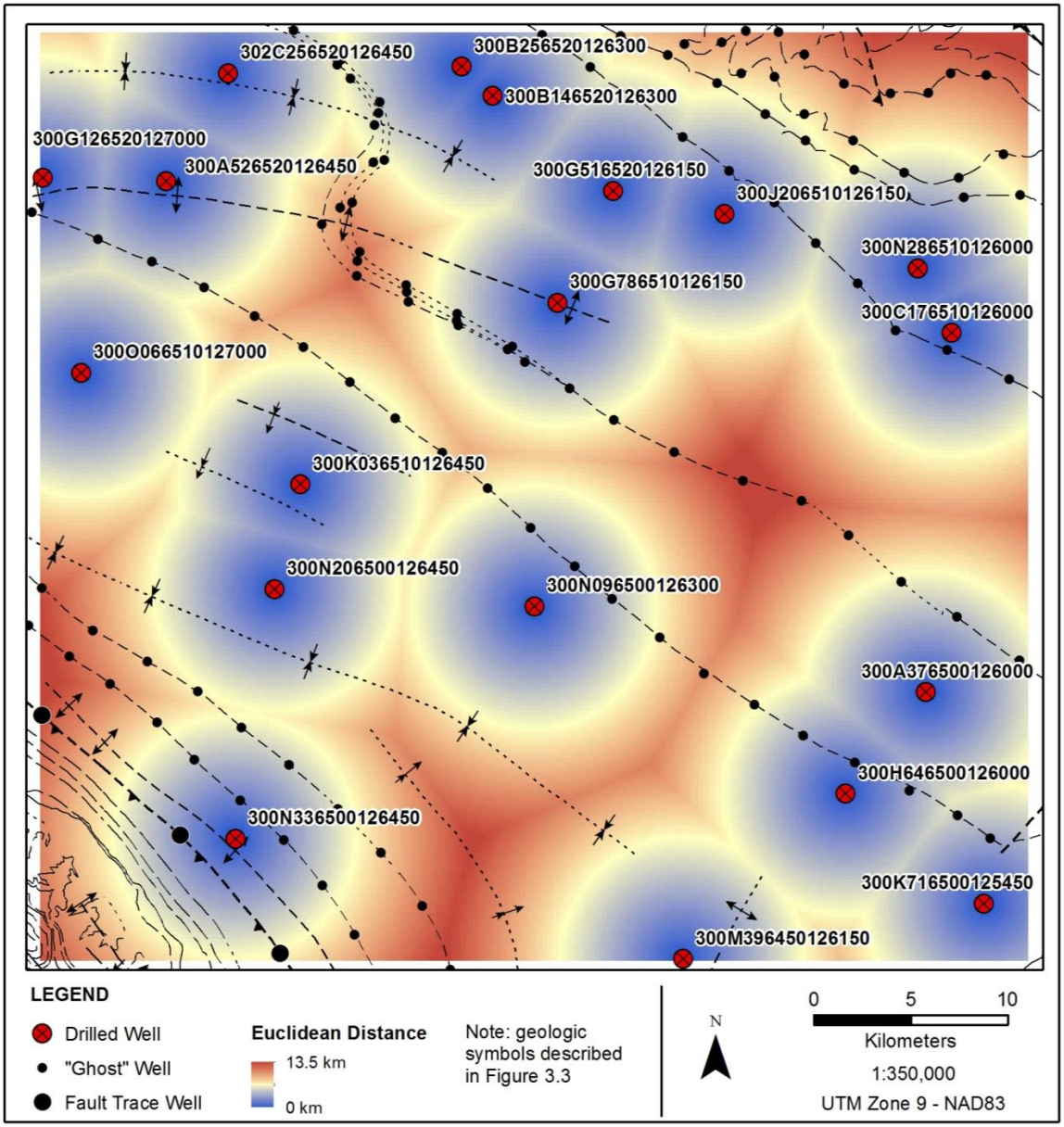

Figure 6.20. Uncertainty map showing distance from control points/wells.

7.0 DISCUSSION

In this section the answers to the research questions are presented. As well, any relevant additional findings are discussed.

7.1 Horizons Method of Modelling

Research Question 1: Using mapped surface geology and sparse boreholes, can we use a modified version of the Horizons Method (Lemon and Jones, 2003) to model the subsurface?

Using the Horizons Method of modelling, it is possible to model the subsurface of an area within the Mackenzie Plain. However, additional control points were necessary in order to better constrain key geologic structures within the area, and some structures were still not captured in the correct location. A fair number of manual edits were also necessary to create a geologically realistic surface. Whether or not the result can be considered an acceptable subsurface model is a subjective answer and depends on the level of geologic certainty and detail required. This model was not considered to be a "reliable" subsurface model, using the reliability criteria defined in Section 5.3.3: Results Assessment.

With the Horizons Method, surfaces are built from the bottom up, with the deepest unit serving as the starting point. The deepest unit is not necessarily the best-constrained surface. In fact, for most of the boreholes within this study area, the depths of the deepest unit, Saline River and below, were mostly inferred depths, rather than measured depths from the wells. It may not be logical in all instances, to eliminate gaps and overlaps in surfaces by setting the bottom surface to the top of an extrapolated surface below. It may be a better idea to start with the best constrained surface, and build surfaces down, or up from this surface, depending on the circumstance. For example, in this study, the Hume Formation had a very identifiable seismic signature, and a gridded surface for the top of the Hume Formation was available which was considered to be an accurate representation. With the knowledge from wells and literature that the Hume Formation thickness does not vary greatly across the study area, we could alternatively build horizon surface elevations both top down and bottom up from the top Hume surface.

Another method, rather than to build the tops and bottoms of surfaces and extrude depths from these, would be to interpolate the thickness of units independently, in a fashion similar to a methodology proposed by Tremblay et al. 2010, with Quaternary stratigraphic units. It would be necessary to know where in space these thickness units existed. However, if that was known, this would be a plausible method. This could be done by adding or subtracting the calculated thicknesses onto another base surface of known location (such as the Hume Formation). This method may be effective at eliminating unwarranted undulations or changes in thickness values due to incorrectly modelled unit tops and bottoms.

A limitation of the methodology used in this study is the prevalence of manual edits that were necessary. This reduces the ability for quick updates should new data become available. With an increase in manual edits, and estimations of well depths, the model simply becomes a visualization of the modeller's interpretation of the subsurface, rather than a mathematical model. The modelling process cannot be executed without geological knowledge, or knowledge about the intricacies of interpolation algorithms. In areas where complex geologic structures exist, without control points constraining the extremities, manual intervention is almost impossible to avoid. Therefore, a methodology such as the Horizons Method, allows a "first pass" at capturing the main geologic structures, and further refinements can then be performed. The solid model structure allows for any level of manual edits and almost any level of geologic complexity (Lemon and Jones, 2003).

7.2 Representation of Structures in the Subsurface

Research Question 2: What does the subsurface of our study area in the Mackenzie Plain look like in three dimensions, using the methodology above?

The subsurface of our study area is presented in Figure 6.18. Comparing the cross-section of the modelled subsurface with the seismic image of the subsurface (Figure 6.20), we can see that the general trend of the dipping beds is captured. The two main prominent features are visible, and it was not surprising that the smaller features such as monoclinal bends in between were not captured – there were no data points or well control in the subsurface providing supporting evidence of these features. The location of the syncline trough, however, was slightly off the true location. This is because the lowest point in a model, using triangulation, will be

captured at a location of a control point – surfaces will not extend above or below control points. Therefore the lack of control points through the bottom of the syncline prevents the precise modelling of the fold position

Research Question 3: What kind of input data can help constrain the spatial location of key geologic structures such as faults and folds?

There are several ways in which we could constrain, or refine, the spatial location of structures such as folds. These structures are determined by observations (e.g. on seismic lines or in the field), and where observations do not exist and extrapolation is necessary, geologic principles are used. Unless a modelling algorithm can incorporate all these rules, we cannot expect it to know the point of inflection of a fold, without telling it. Therefore, as long as the general trend was captured via the modelling from drilled wells only, if a well with inferred depths were placed at the location of the inflection, the model would accurately reflect the position of the fold trough or crest. This would be one method to help constrain the folded features.

Using the Horizons Method, almost any type of geological data could be discretized into points and used in this modelling process to further control structures. Examples include outcrop observations, structural measurements or drawn cross-sections. There is no limit to the type of relevant data that can be used to improve the modelling process; we are only limited by the constraints of the methodologies or software programs chosen.

Incorporating more seismic data is likely the most effective method to control the position of structures in the subsurface. Creating additional wells with depths extracted from the seismic data, particularly at surface contacts, would be expected to be an effective method in this modelling exercise. Seismic data, however, requires additional interpretation to be usable, and is often not as readily available as it is in this area.

Another method commonly used to capture structures in the subsurface is through the use of cross-sections (Keller et al. 2011). The entire model can be built primarily by cross-sections, requiring effort to be put into creating several representative cross-sections across a region, or they can be used to enhance models built using a different method, such as the Horizons Method. Using either technique, points in the cross-

section can be discretized, assigned a Horizon ID in the case of the Horizons Method, and serve as control points for the interpolation process.

Faults pose additional problems in mapping because they represent an abrupt change in a surface and are impossible to model via boreholes only. The orientation of faults and their effect on the intersecting horizons are not easily predicted by a statistical algorithm or mathematical rule set – there are too many exceptions to rules. Normal and vertical faults are generally straightforward to model and simply increase model complexity. Certain software programs may have built in algorithms to deal with these faults automatically in the interpolation process, using a variety of methods. For example, the Spine with Barriers function within ArcGIS has been used successfully, where the fault line from structural maps serve as the barrier in the interpolation of surfaces (Popovs et al., 2015). Rockworks also allows for the creation of geometry-complex faults and for them to serve as an interpolation barrier with a set distance multiplier to show the offset (Rockware17, 2016). Exact methods and algorithmic details of these software functions are often not available to the general public, therefore their appropriateness cannot comprehensively be assessed (Natali et al., 2013).

Thrust faults, or any other geological scenario that requires a single horizon to be fault repeated or folded over itself (i.e. repeated in the vertical plane), are a problem in gridded surface modelling. When dealing with raster surfaces, such as in the interim steps before the final voxel model, it is not possible for a single surface to have two elevation locations (i.e. z values) for a single feature, at the same x, y location In this study, this problem was rectified by creating two separate models on either side of the fault, and only merging them once they were converted into a voxel model format. Voxel models, being true 3D models, allow data to be stored in this manner.

7.4 Interpolation Methods

Research Question 4: What is the most suitable algorithm for interpolating stratigraphic surfaces, given the data available and geologic structures being represented?

The most appropriate interpolation method in this study was determined to be triangulation. Although there were aspects of the other algorithms that were visually pleasing and geologically realistic, particularly the smoothness of surfaces they

produced, these positives did not outweigh the negatives. The negatives in this case are the increase in thicknesses where the input data did not warrant it, or the high and low "bullseyes" in both the thickness and elevation grids, which are uncharacteristic of natural geological systems. Those bullseye effects are caused by the heavy influence of a control point on its direct surroundings, and the fact that maximum and minimum values in the interpolated surface can only occur at sample data points. This results in small peaks and pits around the sample data points. The suggestion of interference folding that these bullseyes produce is not consistent with the geological characteristics of this study area.

Triangulated surfaces are based on topological structures. Their appropriateness, or accurateness in predicting surfaces, is directly related to the logical consistency of the triangular structure. That is, whether or not the formation of the triangles complies with the geological shape of the surface being modelled is the key issue (Weibel and Heller, 1991; Turner, 2006). This is best illustrated by the occurrence of an "edge effect" often seen in triangulated datasets – where there is a drastic increase or decrease in the thickness of a unit, or the shape changes abruptly. This is due to the creation of elongated triangles, at the edge of study areas, due to a lack of evenly distributed control points. An obvious edge effect was not noticeable in these results, however improving the distribution within the study area could also result in improved surfaces. One possibility would be to strategically place inferred wells at locations that would allow a geologically logical triangular structure to be created. Simply creating more points closer together, such as along contact lines, does not necessarily enhance the interpolation. The strategic placement of such inferred points should allow for the desired structures to be modelled.

IDW did not produce models as pleasing as those produced by triangulation because it takes into account distance correlation only. It would have performed better modelling a set of features which vary more predictably with distance. The spatial location of geologic surfaces, however, is generally not a function of distance, rather it is a function of a more complex, and less predictable set of variables including erosion, non-deposition, deformation, etc.

Many studies support the use of kriging for geologic applications. The fact that it adjusts the weights of the surrounding values based on their spatial arrangement, rather than

assuming a single value, is very desirable (Mallet, 2002; Rockware, 2016). The results of this study, however, support the suggestion that kriging performs poorly with discontinuous strata. The surfaces that were continuous, performed well with kriging, however the three surfaces which pinched out below the surface, did not. It is possible the neighbourhood search location was the cause for the poorly interpolated surfaces. The neighbourhood location chosen has also been shown to affect the continuity of a surface – if the change in data from one neighbourhood to the next is too abrupt, or their shape is very rough, discontinuities in the resulting interpolated surface may occur, as the mean is assumed to be constant (Lam, 1983; Meyer, 2004). This can also be considered an artefact of poor data density – should more data points exist, the change may not have been so abrupt.

Kriging is a complex algorithm and there are many parameters that can be changed. As each surface (both top and bottom of each formation) is modelled separately, the optimal variogram and other model parameters may differ for each surface. Finding the optimal set of parameters for one particular dataset is a study in itself. It is possible that kriging could have yielded more acceptable results in the hard-to-model surfaces if more model parameters had been tested. Another method to improve the kriging interpolation may have been to imagine the formation surfaces as being continuous, and extending them beyond the surface (by inferring control points), to not interrupt the interpolation. These surfaces could then be clipped to the DEM. The kriging interpolation algorithm may also simply not be robust enough to incorporate the sharp edges of discontinuities (Stephenson et al. 2003).

One interpolation method that was not tested here was Spline interpolation. This was not tested because it is not considered as common in geological modelling, and was not offered as an option in Rockworks17 (Mei, 2014). This method essentially bends a curvilinear surface to fit the known point values (ArcGIS, 2016). With this method, values can be estimated above or below the maximum and minimum values found in the sample data. This could potentially assist in properly modelling the location of folds in the subsurface, if sufficient data points existed to “bend” the surface at the correct locations.

Interpolation methods are only as good as the data that goes into them. Certain conditions must be satisfied in order to confidently create an accurate interpolation result, the particular set of conditions differing depending on the algorithm chosen. The distribution of control points is a core factor in a successful interpolation, with a higher density of control points needed in areas of increased geological complexity. Boreholes, the most valuable subsurface control, are strategically drilled into formations of economic interest, and not necessarily to ensure an even distribution of subsurface observations across a region. Surface geologic mapping, although useful and likely the most readily available, only gives information about one intersection or contact at each location and limits control points to be clustered along a linear feature. These surface control points force a single unit to a depth of 0 (i.e. 0 thickness), however its location in the subsurface may not be correct. This is why, for example in the folded section in the north part of the model, where Martin House and Arctic Red pinched out, there were sharp, jagged changes in elevation – the top and bottom surfaces were forced to the surface, however the shape of the folded structure in the subsurface is not addressed.

There is no best interpolation algorithm that is superior to all others and appropriate for all geological scenarios. Rather the best algorithm will depend on the sampling process, and the desired features/structures to be modelled. The diversity in conclusions from different studies of this type supports this fact. It is also supported by the results in this study, where some surfaces were modelled well by one algorithm, but other surfaces were not modelled well by the same algorithm – depending on their structure (e.g. thin units).

7.3 Model Uncertainty and Errors

Of the three main components contributing to uncertainty within a geologic model (data density, data quality and geologic complexity), only data density was assessed in this study (Lelliott et al., 2009), and is therefore not sufficient for a comprehensive review of uncertainty. The data density requirements rely heavily on the geological complexity of an area. Widely spaced wells would be sufficient to model an area which is dominated by uniformly dipping bedding with no complex geologic structures; whereas areas of rapid or uneven changes in depth or orientation require a higher number of control points (e.g. wells). Taking into account geologic complexity would be a great improvement to this uncertainty assessment. Data quality is the third main component

often contributing to an uncertainty assessment (Lelliot et al. 2009). This can increase the complexity of an accuracy assessment enormously, especially if a wide variety of sources were used. Mapped surface contacts themselves have a level of uncertainty (defined, approximate, or inferred), which could be incorporated via assigning different weightings or uncertainty buffer zones. It should also be noted that the uncertainties can differ between horizons. This can occur due to not only the difficulty in identifying certain contacts from the wells or seismic data in the subsurface, but also because when incorporating surface-only contacts (e.g. points along a mapped surface contact), uncertainty is low for the two units on either side of the contact, but uncertainty increases for those below for which no data exists. These measures are all important components to take into account for an uncertainty assessment, however were beyond the scope of this study.

Research Question 5: Identify the significant identifiable sources of error in the model, and possible mitigation strategies

With any type of multi-source data integration, the introduction of error from any source, at any stage of the data integration process, is possible. Given that the main data input is drilled well data and inferred depths, the main source of error from inputs would be from incorrect stratigraphic contact picks or the assumptions made for the inferred depths (e.g. the Hume formation has a consistent thickness). In this study, the contacts picks in the wells were all verified and updated by the same geologist, thereby eliminating (to the extent possible), at minimum, the inconsistencies in the picks. Incorrect assumptions regarding unit thicknesses are difficult to mitigate given that those assumptions are based off regional geologic knowledge. However, in this model, the assumptions are explicitly stated, thereby allowing for easy updates, should the knowledge change.

Incorrect surface mapping would also introduce errors. Ensuring subsurface data was incorporated in the surface mapping would reduce this possibility (i.e. the unit at the surface in a borehole matches the mapped surface unit), but if it was not, the modelling process will hopefully assist in identifying those incorrectly mapped areas.

Discrepancies could also exist between ground surface elevations as calculated from the DEM, and the surface elevation as measured in the drilled wells. In this study, a separate DEM was used to clip the modelled surfaces, to ensure an accurate

representation of the ground surface and to serve as the top extent of the model. In mountainous areas with abrupt changes in elevation, such as in the northeast and southeast corners of this study area, incorrect elevations, or elevations that are inconsistent between the two inputs, could result in a completely different unit outcropping at the surface. In this study, this was unlikely to be an issue as there were very few wells in high elevation areas, where this discrepancy would be obvious. Nevertheless, to mitigate the potential for inconsistencies, the surface elevations from the wells were adjusted to match those from the DEM. The subsurface picks, as they were provided as a depth from surface measurement, were updated to reflect the updated surface elevation. As over half the wells were drilled prior to the 1980's, and several in the 1940's or earlier, it was assumed that the well provided elevations would not be more accurate that the current DEM. Depending on the methods used to calculate surface elevation, this may not be the case, particularly with more recently drilled wells. However, no well elevations in this study area differed so significantly that this would be an issue.

It is also possible that gross errors exist in modelling the subsurface simply due to lack of data. Data inputs could be free of error, yet errors in the final model introduced due to a poor interpolation. Data in the subsurface in this study area was sparse, which likely led to an over simplification of structures and even an underestimation of uncertainties. It was shown to result in the incorrect placement of fold troughs. This error is caused by an inappropriate number of inputs, or an unrealistic expectation of the type of structures possible to model, given the available data. With wells in this study area sometimes over 5 kilometers apart, it is unrealistic to expect that small monoclinal bends be captured. It is suggested that a more rigorous analysis be performed at the beginning of the modelling process, on which structures are possible to visualize given data available and the geologic complexity. The sparse datasets here led to a simplification of structures, however, if an assessment had been performed at the beginning, it may have been recognized that it was not feasible to capture those structures. If it was required these features be captured, additional control points could have been added.

In terms of model reliability, the two criteria clearly not met were geologic accuracy and reproducibility. The degree to which the model is "accurate" depends on the final use of this model, and suggestions have been made here to increase the accuracy,

allowing it to conform better to the known subsurface geology. The reproducibility of this model is limited by the number of manual edits and user inferences made in estimating unit thicknesses. However, if geologic principles were followed and the most up-to-date geologic knowledge about the region used, these inferences and manual edits should be very similar in future iterations. Differences should only occur if new geologic information becomes available (e.g. a new measured section).

Voxel models can display almost any complex shape – their effectiveness is only limited by the defined cell size and if it is small enough to effectively capture that shape (Natali et al., 2006). However, undesired visual artefacts can also result due to this discretization of space. Again, this is not an error of the model itself, unless an inappropriate cell size is used and the model user is not aware of its limitations. A smaller cell size in the resulting voxel model of this study, would have been desirable, but was not possible due to time limitations and computational requirements.

7.5 Modelling with Sparse Data and in Other Regions

Lack of data density is a difficult problem to overcome. In the absence of adequate data control, a great deal of freedom is given to the modeller and different interpretations are possible. The model becomes a subjective visualization of what the modeller sees in the subsurface, rather than a result of objective observational measurements and statistical results. It is easy for a geologist to visualize the subsurface, however converting the geological laws used in their own visualization into set modelling rules, is a challenge. The results of this study showed that the number of well control points provided were alone not sufficient to create a reasonable model, and additional inferred control points on contacts and on faults were necessary. It is probable that more structural measurements (such as strikes and dips along folds) could also serve as constraints, in lieu of the inferred control points.

This method could be applied in other areas of similar geologic settings as many of the difficulties and conclusions presented in this study are applicable to areas outside of the Mackenzie Plain. The accurate representation of structures in the subsurface is mainly limited by data density and the optimal placement of control points. Highly deformed areas, such as those with overturned or recumbent folds, would be possible to model with this methodology, however it would require the study area be partitioned into several different sub-models. This partitioning greatly increases the complexity of the

model and the number of controls required to model each fold or fault. It also increases the potential for error introduction, or undesirable visual artefacts, should the cell size be large. Therefore, extreme care should be taken when modelling these sorts of areas, and additional control points at known points of inflection or the extremities of subsurface structures will be essential. Faults present problems in any modelling exercise, however, and their representation and relationship with intersecting horizons has been the focus of several different papers (Maxelon et al., 2009; Wu et al., 2015).

In general, this methodology is extremely robust and can be applied to a wide variety of geologic contexts. It is suggested to only use this methodology in areas where there are no more than a few faults or overturned folds. In regions of simpler geology, such as gently dipping horizons, without the presence of discontinuous strata or complicated folds, this methodology would be extremely simple and effective. A model produced in this sort of region would likely not require any extensive manual edits, if any.

7.6 Final Thoughts

The final model has merit in itself, however the entire model-building process was also found to be useful at identifying problems in the surface mapping. This was found when the interpolation of surfaces did not behave as expected, such as a modelled surface extending way beyond the mapped surface contact. In fact, the surface geology in this study area was updated, to reflect some illuminated discrepancies. This highlights the importance of the whole iterative process of 3D model building. 3D modelling should not be considered an end product; rather, the entire process is a means of studying the subsurface in the modelled region, and allowing for future refinements on the interpretations.

The subsurface features of an area can also be very difficult for non-specialists, and even specialists, to visualize. The resulting model could serve as a visualization tool, even if some features have been simplified. These simplifications, and the limitations of the model, just need to be clear to ensure an appropriate use of the model.

Using statistical algorithms to predict the shape of geological structures that do not follow statistical rules is a challenging task. Geological laws need to be converted to modelling concepts, which will aid in dealing with a variety of scenarios encountered, such as missing strata due to non-deposition or erosion. Once tested and validated, these

rules could serve as the base for future automation of the processes. It is unlikely that these models will ever be fully automated – there rarely exists enough sampled observations, and exceptions to the geologic rules often exist.

A suggestion for future studies would be to examine the effect of strategically placing control points, rather than simply increasing the number of points, particularly with triangulation. What is the optimal distribution structure to model what features? This would allow for future modellers/geologists to understand where their efforts of deducing thicknesses are best used.

8.0 CONCLUSION

In this study, a methodology for creating stratigraphic horizons in three-dimensions, from borehole data, was developed for a region within the Mackenzie Plain, in the Northwest Territories of Canada. Its suitability for 3D modelling in this sedimentary region, with the presence of faulting and folding, was assessed. Three different interpolation algorithms (IDW, kriging and triangulation) were tested to determine which produced the most geologically plausible surfaces. Techniques for refining geological structures in the subsurface, with a lack of dense data, were also presented.

The results of this study showed that it is possible to model the subsurface of the study area, with the addition of several strategically placed boreholes to help constrain the location of the subsurface structures. The main downfall of the modified Horizons Method was the requirement for manual edits to be performed and for additional controls to be added to achieve an accurate representation, which reduces the potential for automation and replication of the model.

To further improve the model, more geological constraints should be incorporated into the model, such as placing controls at the point of inflection on folds, or setting maximum or minimum thicknesses for the horizons. It would be possible to apply these methods to an area of more complex geology. However, it would likely require a significant amount of manual edits, or inferred control points, should more measured inputs not exist for that location. In terms of interpolation stratigraphic surfaces, triangulation yielded the best results of the three methods tested.

Even though the final model was not considered to be a completely accurate and reliable representation of the subsurface, it could be used as a basis for further modelling and further model refinements. In areas of low data density or structural measurements, modelling can serve as a test of proposed subsurface interpretations proposed by the modeller/geologist as it may not generate a “true” picture of the subsurface. An objective/observations-based subsurface model can only be generated with higher density data.

As can be seen here and in other literature, there are many different methods of 3D modelling. The methods chosen depend primarily on the type of data available, what is

being modelled, and where the most time can be invested. Continued research on methods will allow us to apply the most appropriate methods in any given scenario, from the beginning of the modelling process, as well as reduce the chance of error introduction. This will reduce time spent on inappropriate methods, as well as reduce risk of errors.

At present, a great deal of work is required in order to produce geologically accurate three-dimensional models. With more research on exactly what is required to model specific types of features, the amount of work invested will be reduced. This will increase the economic feasibility of creating models, and encourage even the most skeptical geoscientist that these models have merit – hopefully promoting the more widespread use of these models.

9.0 REFERENCES

Aitken, J.D. and D.G. Cook. 1974. Carcajou Canyon map-area, District of Mackenzie, Northwest Territories. Geological Survey of Canada, Paper 74-13, 28 pp.

Calgcagno, P., J.P. Chilès, G. Courrioux and A. Guillen. 2008. Geological modelling from field data and geological knowledge Part 1. Modelling method coupling 3D potential-field interpolation and geological rules. *Physics of the Earth and Planetary Interior* 171: 147-157

Caumon, G., P. Collon-Drouaillet, C. Le Carlier de Veslud, S. Viseur and J. Sausse. 2009. Surface-based 3D modeling of geological structures. *Mathematical Geosciences* 41: 927-945

Dag, A. and A.C. Ozdemir. 2013. A comparative study for 3D surface modeling of coal deposit by spatial interpolation approaches. *Resource Geology* 63: 394-403.

Dhont, D., P. Luxey, and J. Chorowicz. 2005. 3-D modeling of geology maps from surface data. *American Association of Petroleum Geologists Bulletin* 89: 1465-1474.

Fernandez, O., J.A. Muñoz, P. Arbués, O. Favilene and M. Marzo. 2004. Three-dimensional reconstruction of geological surfaces: An example of growth strata and turbidite systems from the Ainsa basin (Pyreneees, Spain). *AAPG Bulletin* 88: 1049-1068

Fisher, T.R. and R.Q. Wales. 1990. 3-D solid modeling of sandstone reservoirs using NURBS – a case study of Noonen Ranch field, Denver basin, Colorado. *Geobyte* 5: 39-41

Frank, T., A-L. Tertois and J-L. Mallet. 2007. 3D-reconstruction of complex geological interfaces from irregularly distributed and noisy point data. *Computers & Geosciences* 33: 932-943

Huang, M., D. Li, and X. Han. 2014. A Stratigraphic modeling method based on borehole data. *IJCSI International Journal of Computer Science* 11: 39-43

Jean, G.A., Yarus, J.M., Flach, G.P., Millings, M.R., Harris, M.K., Chamers, R.L. and F.H. Syms. 2004. Three-dimensional geologic model of southeaster Tertiary coastal-plain sediments, Savannah River Site, South Carolina: An applied geostatistical approach for environmental applications. *Environmental Geosciences* 11: 205-220

Kaufmann, O. and T. Martin. 2008. 3D geological modelling from boreholes, cross-sections and geological maps, application over former natural gas storages in coal mines. *Computers & Geosciences* 34: 278-290

Keefer, D. A. and S. Rittenhouse. 2005. Estimating the uncertainty of 3D geologic maps. Three-Dimensional Geologic Mapping for Groundwater Applications – Workshop Extended Abstracts, Geological Survey of Canada, Open File 5048*:* 31-35.

Keefer, D.A., H. Kessler, M. Cave and S.J. Mathers. 2011. Chapter 2: Major Mapping and Modeling Issues in. Synopsis of Current Three-dimensional Geological Mapping and Modeling; in Geological Survey Organizations. Illinois State Geological Survey Circular 578, Champaign, Illinois: 6-10

Keller, G., G. Matile and H. Thorliefson. 2011. Chapter 11: Manitoba Geological Survey: Multi-scaled 3-D Geological Modeling with a Single Software Solution and Low Costs; in Synopsis of Current Three-dimensional Geological Mapping and Modeling; in Geological Survey Organizations. Illinois State Geological Survey, Circular 578, Champaign, Illinois: 60-63

Kiš, I.M. 2016. Comparison of ordinary and universal kriging interpolation techniques on a depth variable (a case of lineary spatial trend), case study of the Šandrovac Field. *The Mining Geology Petroleum Engineering Bulletin* 2016: 41-58

Lelliott, M.R., M.R. Cave and G.P. Wealthall. 2009. A structured approach to the measurement of uncertainty in 3D geological models. Quarterly Journal of Engineering Geology and Hydrogeology 42: 95-105

Lemon, A.M. and N.L. Jones. 2003. Building solid models from boreholes and user-defined cross-sections. *Computer & Geosciences* 29: 547-555

Lu, G.Y. and D.W. Wong. 2008. An adaptive inverse-distance weighting spatial interpolation technique. *Computers & Geosciences* 34: 1044-1055

Luo, W., Taylor, M.C., Parker, S.R. 2008. A comparison of spatial interpolation methods to estimate continuous wind speed surfaces using irregularly distributed data from England and Wales. *International Journal of Climatology* 28: 947-959

MacCormack, K.E. 2010. Improving the accuracy of 3d geologic subsurface models. PhD thesis. Hamilton, Canada: McMaster University

MacCormack, K.E. and C.H. Eyles. 2012. Assessing the impact of program selection on the accuracy of 3D models. *Geosphere* 8: 534-543

MacLean, B.C., 2011. Tectonic and stratigraphic evolution of the Cambrian basin of northern Northwest Territories, Bulletin of Canadian Petroleum Geology 59: 172-194.

MacLean, B.C. 2012. GIS-enabled structure maps of subsurface Phanerozoic strata, northwestern Northwest Territories; Geological Survey of Canada, Open File 7172. doi:10.4095/292152

Mallet, J-L. 1992. *Geomodeling*. New York: Oxford University Press.

Marinoni, O. 2003. Improving geological models using a combined ordinary-indicator kriging approach. Engineering Geology 69, 37-45

Mei, G. 2014. Summary on Several Key Techniques in 3D Geological Modeling. The Scientific World Journal, 2014, Article ID 723832, 11pp. doi:10.1155/2014/723832

Natali, M., E.M. Lidal, J. Parulek, I. Viola and D. Pate. 2013. Modeling Terrains and Subsurface Geology. *Eurographics* 2013: 155-173

National Energy Board. 2016. Frontier Information Office Services. Retrieved December 12, 2016 from https://www.neb-one.gc.ca/nrth/frntrffc-eng.html

Passey, S.R. and T. Varming. 2010. Surface interpolation within a continental flood basalt province: An example from the Palaeogene Faroe Islands Basalt Group. *Journal of Structural Geology* 32: 709-723

Pope, M.C. and S.A. Leslie. 2013. New data from Late Ordovician-Early Silurian Mount Kindle Formation measured sections, Franklin Mountains and eastern Mackenzie Mountains, Northwest Territories; Geological Survey of Canada, Current Research 2013-8, 11pp. doi:10.4095/292389

Powell, J., D. Schneider, D. Stockli, and K. Fallas .2016. Zircon (U-Th)/He thermochronology of Neoproterozoic strata from the Mackenzie Mountains, Canada: Implications for the Phanerozoic exhumation and deformation history of the northern Canadian Cordillera, *Tectonics* 35: 663-689, doi:10.1002/2015TC003989

Rockware. 2016. Rockworks17 Software Help. Boulder, CA.

Ross, M., M. Parent and R. Lefebvre. 2005. 3D geologic framework models for regional hydrogeology: a case study from a Quaternary basin of southwestern Quebec, Canada. *Hydrogeology Journal* 13: 690-707

Russell, H.A.J., J. Brodarick, G. Keller, K.E. MacCormack, D.E. Snyder and M.R. St-Onge. 2015. A perspective on a Three Dimensional Framework for Canadian Geology; in *AER/AGS Special Report* 101

Sprague, K.B. and E.A. De Kemp. 2005. Interpretive Tools for 3-D Structural Geological Modelling Part II: Surface Design form Sparse Spatial Data. *GeoInformatica* 9: 5-32

Tacher, L., I. Pomian-Srzednicki and A. Parriaux. 2006. Geological uncertainties associated with 3-D subsurface models. *Computers and Geosciences* 32: 212-221

Thorleifson, L. H. and R.C. Berg. 2002. Introduction - The need for high-quality three dimensional geological information for groundwater and other environmental applications. Geological Survey of Canada, Open File 1449.

Tobler, W.R. 1970. A computer movie simulating urban growth in the Detroit region. *Economic Geography* 46, 234-240

Turner, K. 2006. Challenges and trends for geological modelling and visualisation. *Bulletin of Engineering Geology and the Environment* 65: 109-127

Weber, D.D. and E.J. Englund. 1999. An experiemental comparison of ordinary and universal kriging and inverse distance weighting. *Mathematical Geology* 31 (4), 375-390

Weibel, R. and M. Heller. 1991. Digital Terrain Modelling, in Ch 19. Geographical Information Systems: Principles and Applications: 269-297

Wellman, J.F., F.G. Horowitz, E. Schill, and K. Regenauer-Lieb. 2010. Towards incorporating uncertainty of structural data in 3D geologic inversion. *Tectophysics* 490: 141-151

Wu, Q. and H. Xu. 2003. An approach to computer modelling and visualization of geological faults in 3D. *Computers & Geosciences* 29: 507-513

Wu, Q., H. Xu and H. Zou. 2005. An effective method for 3D geological modeling with multi-source data integration. *Computers & Geosciences* 31: 35-43

Zhang, F., H.H. Zhu and M.X. Ning. 2006. Modeling methods and spatial data model of layered rock-mass. *Journal of China University of Mining and Technology* 33: 103-108

Zhu, L., C. Zhang, M. Li, X. Pan, X and J. Sun. 2012. Building 3D solid models of sedimentary stratigraphic systems from borehole data: An automatic method and case studies. *Engineering Geology* 127: 1-13

APPENDICES

APPENDIX A

Well stratigraphic database

UWI	TOP	BOTTOM	STRATIGRAPHY
300A376500126000	0	157	SLATER RIVER FM
300A376500126000	157	157	MARTIN HOUSE FM
300A376500126000	157	662.9	IMPERIAL FM
300A376500126000	662.9	862.3	HORN RIVER GP
300A376500126000	862.3	996.7	HUME FM
300A376500126000	996.7	1336.7	BEAR ROCK FM
300A376500126000	1336.7	1616.7	FRANKLIN MOUNTAIN
300A376500126000	1616.7	3000	SALINE AND BELOW
300A526520126450	-150	-50	LITTLE BEAR FM
300A526520126450	-50	54	SLATER RIVER FM
300A526520126450	54	114.3	ARCTIC RED FM
300A526520126450	114.3	146.3	MARTIN HOUSE FM
300A526520126450	146.3	678.2	IMPERIAL FM
300A526520126450	678.2	960.1	HORN RIVER GP
300A526520126450	960.1	1091.2	HUME FM
300A526520126450	1091.2	1389.9	BEAR ROCK FM
300A526520126450	1389.9	1707.3	FRANKLIN MOUNTAIN
300A526520126450	1707.3	3000	SALINE AND BELOW
300B146520126300	-400	-290	SLATER RIVER FM
300B146520126300	-290	-280	MARTIN HOUSE FM
300B146520126300	-280	448.1	IMPERIAL FM
300B146520126300	448.1	634	HORN RIVER GP
300B146520126300	634	732.1	HUME FM
300B146520126300	732.1	1032	BEAR ROCK FM
300B146520126300	1032	1250	FRANKLIN MOUNTAIN
300B146520126300	1250		SALINE AND BELOW
300B256520126300	-500	-310	SLATER RIVER FM
300B256520126300	-310	-300	MARTIN HOUSE FM
300B256520126300	-300	401.1	IMPERIAL FM
300B256520126300	401.1	600.2	HORN RIVER GP
300B256520126300	600.2	697.1	HUME FM
300B256520126300	697.1	997.1	BEAR ROCK FM
300B256520126300	997.1	1237	FRANKLIN MOUNTAIN
300B256520126300	1237	2464	SALINE AND BELOW

300C176510126000	-400	-400	MARTIN HOUSE FM
300C176510126000	-400	0	IMPERIAL FM
300C176510126000	-10	0	IMPERIAL FM
300C176510126000	-10	146	HORN RIVER GP
300C176510126000	146	227.1	HUME FM
300C176510126000	227.1	565	BEAR ROCK FM
300C176510126000	565	869.6	FRANKLIN MOUNTAIN
300C176510126000	869.6	2000	SALINE AND BELOW
300G126520127000		-30	LITTLE BEAR FM
300G126520127000	-30	304.8	SLATER RIVER FM
300G126520127000	304.8	365.8	ARCTIC RED FM
300G126520127000	365.8	402.3	MARTIN HOUSE FM
300G126520127000	402.3	940.3	IMPERIAL FM
300G126520127000	940.3	1211.6	HORN RIVER GP
300G126520127000	1211.6	1334.1	HUME FM
300G126520127000	1334.1	1634.1	BEAR ROCK FM
300G126520127000	1634.1	2006.2	FRANKLIN MOUNTAIN
300G126520127000	2006.2	3000	SALINE AND BELOW
300G516520126150	-400	-300	SLATER RIVER FM
300G516520126150	-300	-300	ARCTIC RED FM
300G516520126150	-300	-300	MARTIN HOUSE FM
300G516520126150	-300	365.7	IMPERIAL FM
300G516520126150	365.7	546.5	HORN RIVER GP
300G516520126150	546.5	676.5	HUME FM
300G516520126150	676.5	1026.5	BEAR ROCK FM
300G516520126150	1026.5	1276.5	FRANKLIN MOUNTAIN
300G516520126150	1276.5	2500	SALINE AND BELOW
300G786510126150	-300	-200	SLATER RIVER FM
300G786510126150	-200	-200	MARTIN HOUSE FM
300G786510126150	-200	-200	ARCTIC RED FM
300G786510126150	-200	365.7	IMPERIAL FM
300G786510126150	365.7	546.5	HORN RIVER GP
300G786510126150	546.5	661.4	HUME FM
300G786510126150	661.4	950	BEAR ROCK FM
300G786510126150	950	1407.1	FRANKLIN MOUNTAIN
300G786510126150	1407.1	2500	SALINE AND BELOW
300H646500126000	0	107	LITTLE BEAR FM
300H646500126000	107	390	SLATER RIVER FM
300H646500126000	390	390	ARCTIC RED FM

300H646500126000	390	430	MARTIN HOUSE FM
300H646500126000	430	1133	IMPERIAL FM
300H646500126000	1133	1300	HORN RIVER GP
300H646500126000	1300	1430	HUME FM
300H646500126000	1430	1730	BEAR ROCK FM
300H646500126000	1730	1730	MOUNT KINDLE FM
300H646500126000	1730	2030	FRANKLIN MOUNTAIN
300H646500126000	2030	3000	SALINE AND BELOW
300J206510126150	-300	231.6	IMPERIAL FM
300J206510126150	231.6	320	HORN RIVER GP
300J206510126150	320	450	HUME FM
300J206510126150	450	750	BEAR ROCK FM
300J206510126150	750	970	FRANKLIN MOUNTAIN
300J206510126150	970	2500	SALINE AND BELOW
300K036510126450	0	85.3	LITTLE BEAR FM
300K036510126450	85.3	762	SLATER RIVER FM
300K036510126450	762	875.7	ARCTIC RED FM
300K036510126450	875.7	907.4	MARTIN HOUSE FM
300K036510126450	907.4	1573.6	IMPERIAL FM
300K036510126450	1573.6	1770.6	HORN RIVER GP
300K036510126450	1770.6	1889.2	HUME FM
300K036510126450	1889.2	2313.1	BEAR ROCK FM
300K036510126450	2313.1	2313.1	MOUNT KINDLE FM
300K036510126450	2313.1	2729	FRANKLIN MOUNTAIN
300K036510126450	2729	3000	SALINE AND BELOW
300K716500125450	0	227.7	LITTLE BEAR FM
300K716500125450	227.7	618.1	SLATER RIVER FM
300K716500125450	618.1	618.1	ARCTIC RED FM
300K716500125450	618.1	618.1	MARTIN HOUSE FM
300K716500125450	618.1	1070.2	IMPERIAL FM
300K716500125450	1070.2	1322.5	HORN RIVER GP
300K716500125450	1322.5	1459.9	HUME FM
300K716500125450	1459.9	1760	BEAR ROCK FM
300K716500125450	1760	2045	FRANKLIN MOUNTAIN
300K716500125450	2045	3000	SALINE AND BELOW
300M396450126150	0	100	LITTLE BEAR FM
300M396450126150	100	784.9	SLATER RIVER FM
300M396450126150	784.9	912	ARCTIC RED FM

300M396450126150	912	936	MARTIN HOUSE FM
300M396450126150	936	1550	IMPERIAL FM
300M396450126150	1550	1750	HORN RIVER GP
300M396450126150	1750	1880	HUME FM
300M396450126150	1880	2230	BEAR ROCK FM
300M396450126150	2230	2230	MOUNT KINDLE FM
300M396450126150	2230	2630	FRANKLIN MOUNTAIN
300M396450126150	2630		SALINE AND BELOW
300N096500126300	-50	230	LITTLE BEAR FM
300N096500126300	230	846	SLATER RIVER FM
300N096500126300	846	925	ARCTIC RED FM
300N096500126300	925	950.5	MARTIN HOUSE FM
300N096500126300	950.5	1635.9	IMPERIAL FM
300N096500126300	1635.9	1828.9	HORN RIVER GP
300N096500126300	1828.9	1950	HUME FM
300N096500126300	1950	2300	BEAR ROCK FM
300N096500126300	2300	2300	MOUNT KINDLE FM
300N096500126300	2300	2630	FRANKLIN MOUNTAIN
300N096500126300	2630	3000	SALINE AND BELOW
300N206500126450	0	242.5	LITTLE BEAR FM
300N206500126450	242.5	990	SLATER RIVER FM
300N206500126450	990	1140.3	ARCTIC RED FM
300N206500126450	1140.3	1174.5	MARTIN HOUSE FM
300N206500126450	1174.5	1910.4	IMPERIAL FM
300N206500126450	1910.4	2095.7	HORN RIVER GP
300N206500126450	2095.7	2222	HUME FM
300N206500126450	2222	2572	BEAR ROCK FM
300N206500126450	2572	2572	MOUNT KINDLE FM
300N206500126450	2572	3000	FRANKLIN MOUNTAIN
300N206500126450	3000	3500	SALINE AND BELOW
300N286510126000	-500	0	IMPERIAL FM
300N286510126000	0	143.3	HORN RIVER GP
300N286510126000	143.3	259.4	HUME FM
300N286510126000	259.4	573	BEAR ROCK FM
300N286510126000	573	853.1	FRANKLIN MOUNTAIN
300N286510126000	853.1		SALINE AND BELOW
300N336500126450	-100	0	SLATER RIVER FM
300N336500126450	0	328	ARCTIC RED FM

300N336500126450	328	364	MARTIN HOUSE FM
300N336500126450	364	873	IMPERIAL FM
300N336500126450	873	1046.1	HORN RIVER GP
300N336500126450	1046.1	1172	HUME FM
300N336500126450	1172	1550	BEAR ROCK FM
300N336500126450	1550	1755	MOUNT KINDLE FM
300N336500126450	1755	2200	FRANKLIN MOUNTAIN
300N336500126450	2200	3000	SALINE AND BELOW
300O066510127000	0	50	LITTLE BEAR FM
300O066510127000	50	787	SLATER RIVER FM
300O066510127000	787	926	ARCTIC RED FM
300O066510127000	926	962.5	MARTIN HOUSE FM
300O066510127000	962.5	1625.2	IMPERIAL FM
300O066510127000	1625.2	1806	HORN RIVER GP
300O066510127000	1806	1930	HUME FM
300O066510127000	1930	2280	BEAR ROCK FM
300O066510127000	2280	2280	MOUNT KINDLE FM
300O066510127000	2280	2680	FRANKLIN MOUNTAIN
300O066510127000	2680	3500	SALINE AND BELOW
302C256520126450	-30	170.7	SLATER RIVER FM
302C256520126450	170.7	170.7	ARCTIC RED FM
302C256520126450	170.7	210.3	MARTIN HOUSE FM
302C256520126450	210.3	655.3	IMPERIAL FM
302C256520126450	655.3	909.8	HORN RIVER GP
302C256520126450	909.8	1040	HUME FM
302C256520126450	1040	1340	BEAR ROCK FM
302C256520126450	1390	1668	FRANKLIN MOUNTAIN
302C256520126450	1668	2743	SALINE AND BELOW

APPENDIX B

Variogram settings for kriging of the Hume formation

Spoke Spacing
90.0 degrees.

Spoke Tolerance
+/- 45.0 degrees.

Distance Increment
2,943.7

Distance Tolerance
+/- 1,471.85

Maximum Cutoff Distance
24,605.05

Best Variogram (i.e. Best Correlation)
Exponential Without Nugget

Correlation Coefficient of Best Variogram
0.91

Variogram That Was Actually Used
Exponential Without Nugget

Correlation Coefficient
0.91

Nugget
0.0

Relative Sill
497,937.26

Major Axis Direction
N103.6 degrees.

Major Axis Range
15,009.08

Minor Axis Direction
N193.6 degrees.

Minor Axis Range
10,580.17

Series from Lund University

Department of Physical Geography and Ecosystem Science

Master Thesis in Geographical Information Science

1. *Anthony Lawther:* The application of GIS-based binary logistic regression for slope failure susceptibility mapping in the Western Grampian Mountains, Scotland (2008).
2. *Rickard Hansen:* Daily mobility in Grenoble Metropolitan Region, France. Applied GIS methods in time geographical research (2008).
3. *Emil Bayramov:* Environmental monitoring of bio-restoration activities using GIS and Remote Sensing (2009).
4. *Rafael Villarreal Pacheco:* Applications of Geographic Information Systems as an analytical and visualization tool for mass real estate valuation: a case study of Fontibon District, Bogota, Columbia (2009).
5. *Siri Oestreich Waage:* a case study of route solving for oversized transport: The use of GIS functionalities in transport of transformers, as part of maintaining a reliable power infrastructure (2010).
6. *Edgar Pimiento:* Shallow landslide susceptibility – Modelling and validation (2010).
7. *Martina Schäfer:* Near real-time mapping of floodwater mosquito breeding sites using aerial photographs (2010).
8. *August Pieter van Waarden-Nagel:* Land use evaluation to assess the outcome of the programme of rehabilitation measures for the river Rhine in the Netherlands (2010).
9. *Samira Muhammad:* Development and implementation of air quality data mart for Ontario, Canada: A case study of air quality in Ontario using OLAP tool. (2010).
10. *Fredros Oketch Okumu*: Using remotely sensed data to explore spatial and temporal relationships between photosynthetic productivity of vegetation and malaria transmission intensities in selected parts of Africa (2011).
11. *Svajunas Plunge:* Advanced decision support methods for solving diffuse water pollution problems (2011).
12. *Jonathan Higgins:* Monitoring urban growth in greater Lagos: A case study using GIS to monitor the urban growth of Lagos 1990 - 2008 and produce future growth prospects for the city (2011).
13. *Mårten Karlberg:* Mobile Map Client API: Design and Implementation for Android (2011).
14. *Jeanette McBride:* Mapping Chicago area urban tree canopy using color infrared imagery (2011).
15. *Andrew Farina:* Exploring the relationship between land surface temperature and vegetation abundance for urban heat island mitigation in Seville, Spain (2011).
16. *David Kanyari*: Nairobi City Journey Planner: An online and a Mobile Application (2011).
17. *Laura V. Drews:* Multi-criteria GIS analysis for siting of small wind power plants - A case study from Berlin (2012).
18. *Qaisar Nadeem:* Best living neighborhood in the city - A GIS based multi criteria evaluation of ArRiyadh City (2012).

19. *Ahmed Mohamed El Saeid Mustafa:* Development of a photo voltaic building rooftop integration analysis tool for GIS for Dokki District, Cairo, Egypt (2012).
20. *Daniel Patrick Taylor*: Eastern Oyster Aquaculture: Estuarine Remediation via Site Suitability and Spatially Explicit Carrying Capacity Modeling in Virginia's Chesapeake Bay (2013).
21. *Angeleta Oveta Wilson:* A Participatory GIS approach to *unearthing* Manchester's Cultural Heritage '*gold mine'* (2013).
22. *Ola Svensson:* Visibility and Tholos Tombs in the Messenian Landscape: A Comparative Case Study of the Pylian Hinterlands and the Soulima Valley (2013).
23. *Monika Ogden:* Land use impact on water quality in two river systems in South Africa (2013).
24. *Stefan Rova:* A GIS based approach assessing phosphorus load impact on Lake Flaten in Salem, Sweden (2013).
25. *Yann Buhot:* Analysis of the history of landscape changes over a period of 200 years. How can we predict past landscape pattern scenario and the impact on habitat diversity? (2013).
26. *Christina Fotiou:* Evaluating habitat suitability and spectral heterogeneity models to predict weed species presence (2014).
27. *Inese Linuza:* Accuracy Assessment in Glacier Change Analysis (2014).
28. *Agnieszka Griffin:* Domestic energy consumption and social living standards: a GIS analysis within the Greater London Authority area (2014).
29. *Brynja Guðmundsdóttir:* Detection of potential arable land with remote sensing and GIS - A Case Study for Kjósarhreppur (2014).
30. *Oleksandr Nekrasov:* Processing of MODIS Vegetation Indices for analysis of agricultural droughts in the southern Ukraine between the years 2000-2012 (2014).
31. *Sarah Tressel:* Recommendations for a polar Earth science portal in the context of Arctic Spatial Data Infrastructure (2014).
32. *Caroline Gevaert:* Combining Hyperspectral UAV and Multispectral Formosat-2 Imagery for Precision Agriculture Applications (2014).
33. *Salem Jamal-Uddeen:* Using GeoTools to implement the multi-criteria evaluation analysis - weighted linear combination model (2014).
34. *Samanah Seyedi-Shandiz:* Schematic representation of geographical railway network at the Swedish Transport Administration (2014).
35. *Kazi Masel Ullah:* Urban Land-use planning using Geographical Information System and analytical hierarchy process: case study Dhaka City (2014).
36. *Alexia Chang-Wailing Spitteler:* Development of a web application based on MCDA and GIS for the decision support of river and floodplain rehabilitation projects (2014).
37. *Alessandro De Martino:* Geographic accessibility analysis and evaluation of potential changes to the public transportation system in the City of Milan (2014).
38. *Alireza Mollasalehi:* GIS Based Modelling for Fuel Reduction Using Controlled Burn in Australia. Case Study: Logan City, QLD (2015).
39. *Negin A. Sanati:* Chronic Kidney Disease Mortality in Costa Rica; Geographical Distribution, Spatial Analysis and Non-traditional Risk Factors (2015).

40. *Karen McIntyre:* Benthic mapping of the Bluefields Bay fish sanctuary, Jamaica (2015).
41. *Kees van Duijvendijk:* Feasibility of a low-cost weather sensor network for agricultural purposes: A preliminary assessment (2015).
42. *Sebastian Andersson Hylander:* Evaluation of cultural ecosystem services using GIS (2015).
43. *Deborah Bowyer:* Measuring Urban Growth, Urban Form and Accessibility as Indicators of Urban Sprawl in Hamilton, New Zealand (2015).
44. *Stefan Arvidsson:* Relationship between tree species composition and phenology extracted from satellite data in Swedish forests (2015).
45. *Damián Giménez Cruz*: GIS-based optimal localisation of beekeeping in rural Kenya (2016).
46. *Alejandra Narváez Vallejo:* Can the introduction of the topographic indices in LPJ-GUESS improve the spatial representation of environmental variables? (2016).
47. *Anna Lundgren:* Development of a method for mapping the highest coastline in Sweden using breaklines extracted from high resolution digital elevation models (2016).
48. *Oluwatomi Esther Adejoro:* Does location also matter? A spatial analysis of social achievements of young South Australians (2016).
49. *Hristo Dobrev Tomov:* Automated temporal NDVI analysis over the Middle East for the period 1982 - 2010 (2016).
50. *Vincent Muller:* Impact of Security Context on Mobile Clinic Activities A GIS Multi Criteria Evaluation based on an MSF Humanitarian Mission in Cameroon (2016).
51. *Gezahagn Negash Seboka:* Spatial Assessment of NDVI as an Indicator of Desertification in Ethiopia using Remote Sensing and GIS (2016).
52. *Holly Buhler:* Evaluation of Interfacility Medical Transport Journey Times in Southeastern British Columbia. (2016).
53. *Lars Ole Grottenberg*: Assessing the ability to share spatial data between emergency management organisations in the High North (2016).
54. *Sean Grant:* The Right Tree in the Right Place: Using GIS to Maximize the Net Benefits from Urban Forests (2016).
55. *Irshad Jamal:* Multi-Criteria GIS Analysis for School Site Selection in Gorno-Badakhshan Autonomous Oblast, Tajikistan (2016).
56. *Fulgencio Sanmartín:* Wisdom-volkano: A novel tool based on open GIS and time-series visualization to analyse and share volcanic data (2016).
57. *Nezha Acil:* Remote sensing-based monitoring of snow cover dynamics and its influence on vegetation growth in the Middle Atlas Mountains (2016).
58. *Julia Hjalmarsson:* A Weighty Issue: Estimation of Fire Size with Geographically Weighted Logistic Regression (2016).
59. *Mathewos Tamiru Amato:* Using multi-criteria evaluation and GIS for chronic food and nutrition insecurity indicators analysis in Ethiopia (2016).
60. *Karim Alaa El Din Mohamed Soliman El Attar:* Bicycling Suitability in Downtown, Cairo, Egypt (2016).
61. *Gilbert Akol Echelai:* Asset Management: Integrating GIS as a Decision Support Tool in Meter Management in National Water and Sewerage Corporation (2016).
62. *Terje Slinning:* Analytic comparison of multibeam echo soundings (2016).

63. *Gréta Hlín Sveinsdóttir:* GIS-based MCDA for decision support: A framework for wind farm siting in Iceland (2017).
64. *Jonas Sjögren:* Consequences of a flood in Kristianstad, Sweden: A GIS-based analysis of impacts on important societal functions (2017).